



The FOCI™ method of depth migration

Gary Margrave

Saleh Al-Saleh

Hugh Geiger

Michael Lamoureaux



mitacs

POTSI

π Pacific Institute
for the Mathematical Sciences

Outline

Wavefield extrapolators and stability

FOCI { **A stabilizing Wiener filter**
Dual operator tables
Spatial resampling
Post stack testing
Pre stack testing

Wavefield Extrapolators

The phase-shift extrapolation expression

$$\psi(x_T, z, \omega) = \frac{1}{(2\pi)^{n-1}} \int_{\mathbb{R}^{n-1}} \varphi(k_T, z=0, \omega) \left[e^{ik_z z} \right] e^{-ik_T \cdot x_T} dk_T$$

$\psi(x_T, z, \omega)$ output wavefield

$\varphi(k_T, z=0, \omega)$ Fourier transform of input wavefield

Wavefield Extrapolators

The phase-shift operator

$$e^{ik_z z} = \hat{W}_n(z)$$

$$k_z = \begin{cases} \sqrt{\frac{\omega^2}{v^2} - k_T^2}, & \frac{\omega^2}{v^2} > k_T^2 & \text{wavelike} \\ i\sqrt{k_T^2 - \frac{\omega^2}{v^2}}, & k_T^2 > \frac{\omega^2}{v^2} & \text{evanescent} \end{cases}$$

Wavefield Extrapolators

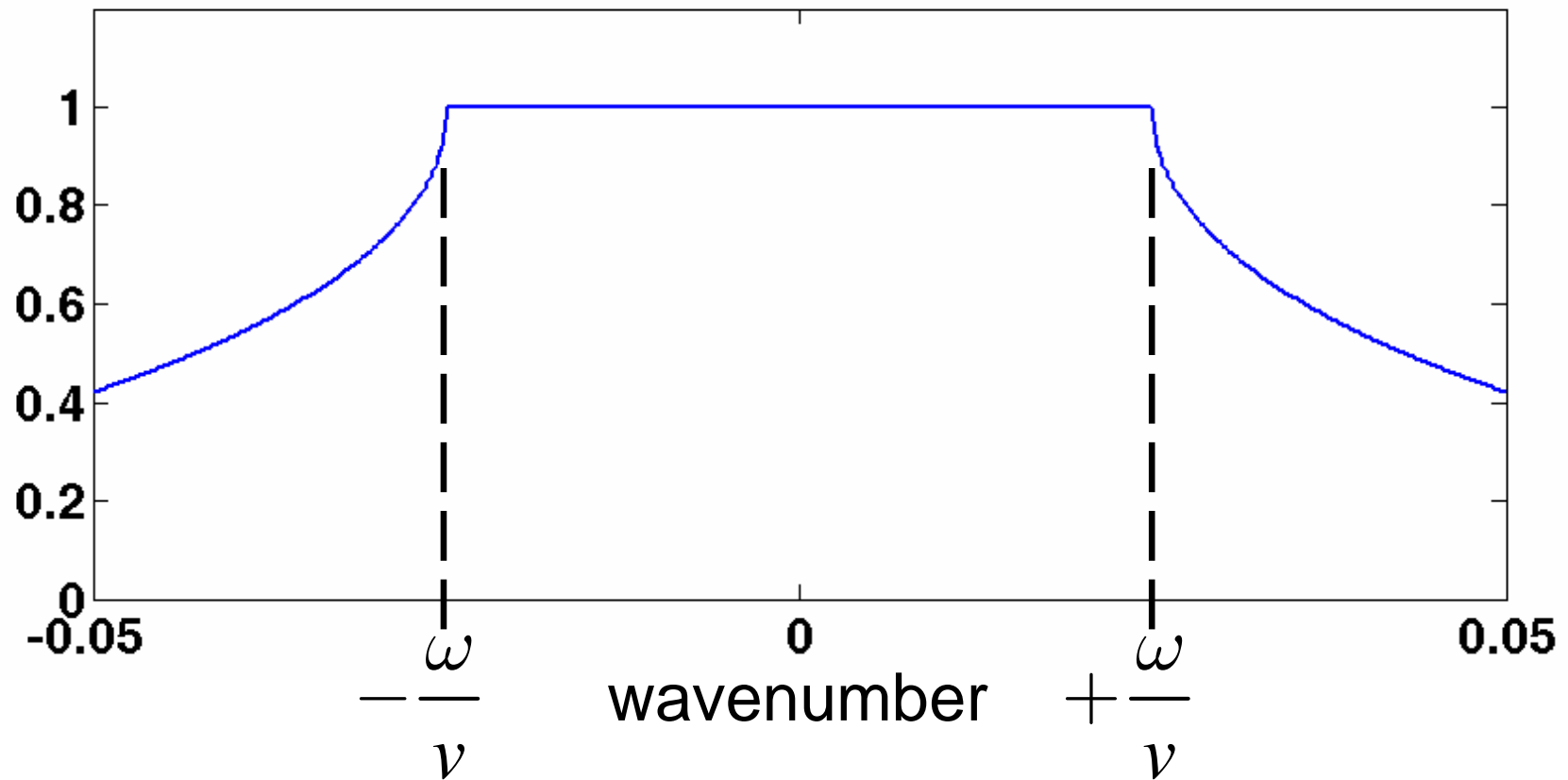
The PSPI extension

$$e^{ik_z z} = \hat{W}_n(z)$$

$$k_z = \begin{cases} \sqrt{\frac{\omega^2}{v(x_T)^2} - k_T^2}, & \frac{\omega^2}{v(x_T)^2} > k_T^2 \\ i \sqrt{k_T^2 - \frac{\omega^2}{v(x_T)^2}}, & k_T^2 > \frac{\omega^2}{v(x_T)^2} \end{cases}$$

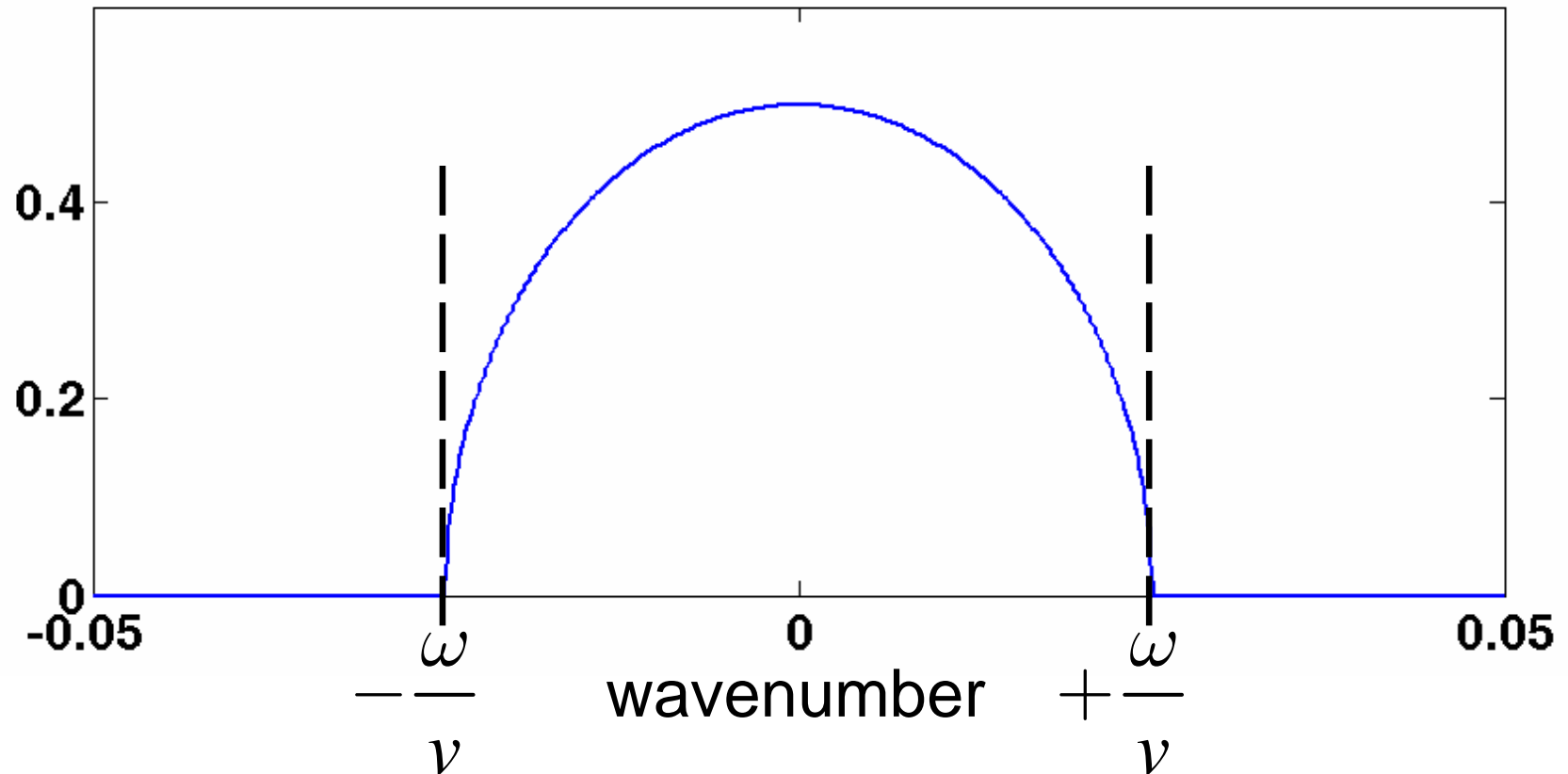
Wavefield Extrapolators

$$|\hat{W}_2(z)|$$



Wavefield Extrapolators

$$\text{phase} \left[\hat{W}_2(z) \right]$$



Wavefield Extrapolators

In the space-frequency domain

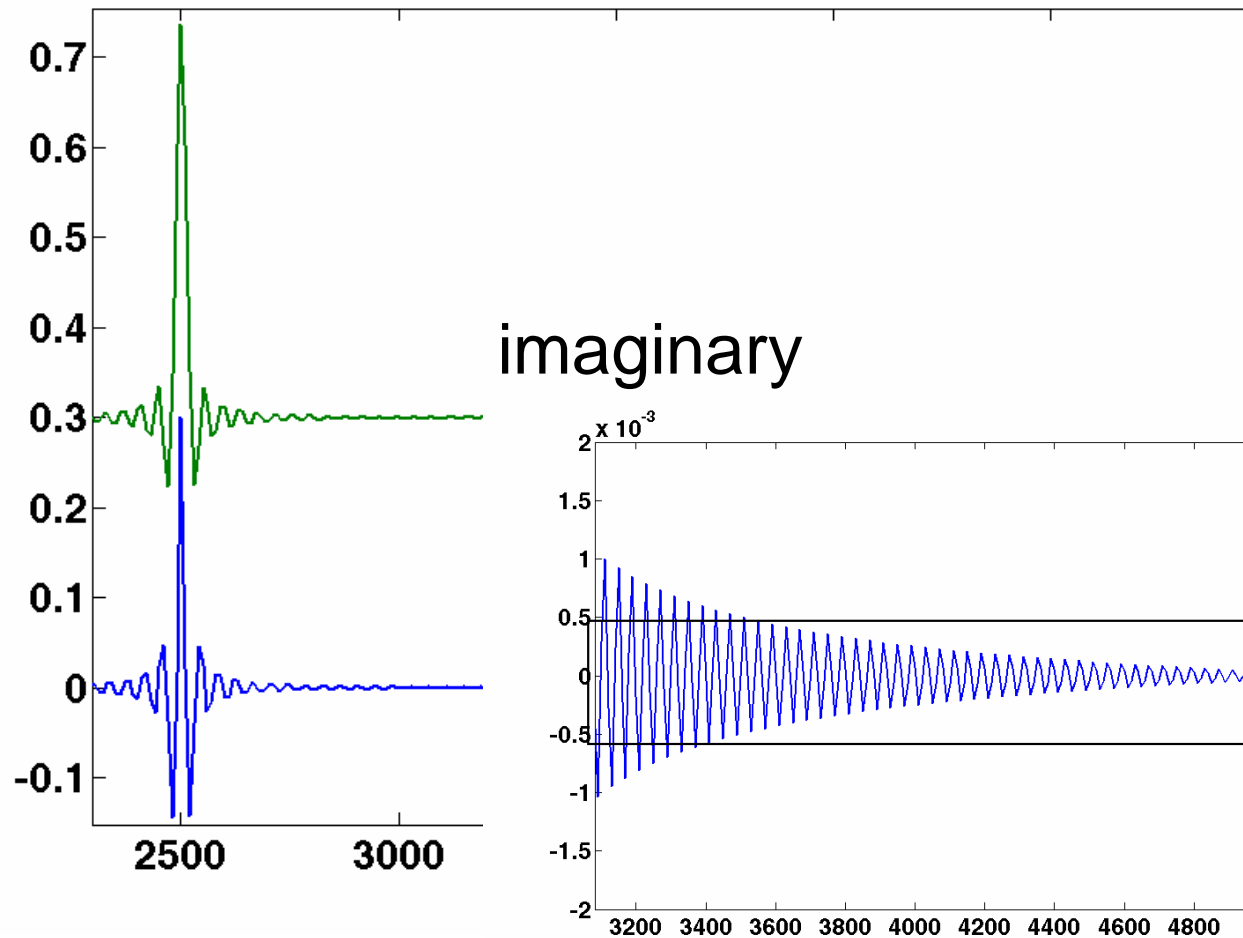
$$\psi(x_T, z, \omega) = \int_{\mathbb{R}^{n-1}} \psi(\hat{x}_T, z=0, \omega) W_n(x_T - \hat{x}_T, z, \omega) d\hat{x}_T$$

where

$$W_n(x_T - \hat{x}_T, z, \omega) = \frac{1}{(2\pi)^{n-1}} \int_{\mathbb{R}^{n-1}} \hat{W}_n(k_T, z, \omega) e^{-ik_T \cdot (x_T - \hat{x}_T)} dk_T$$

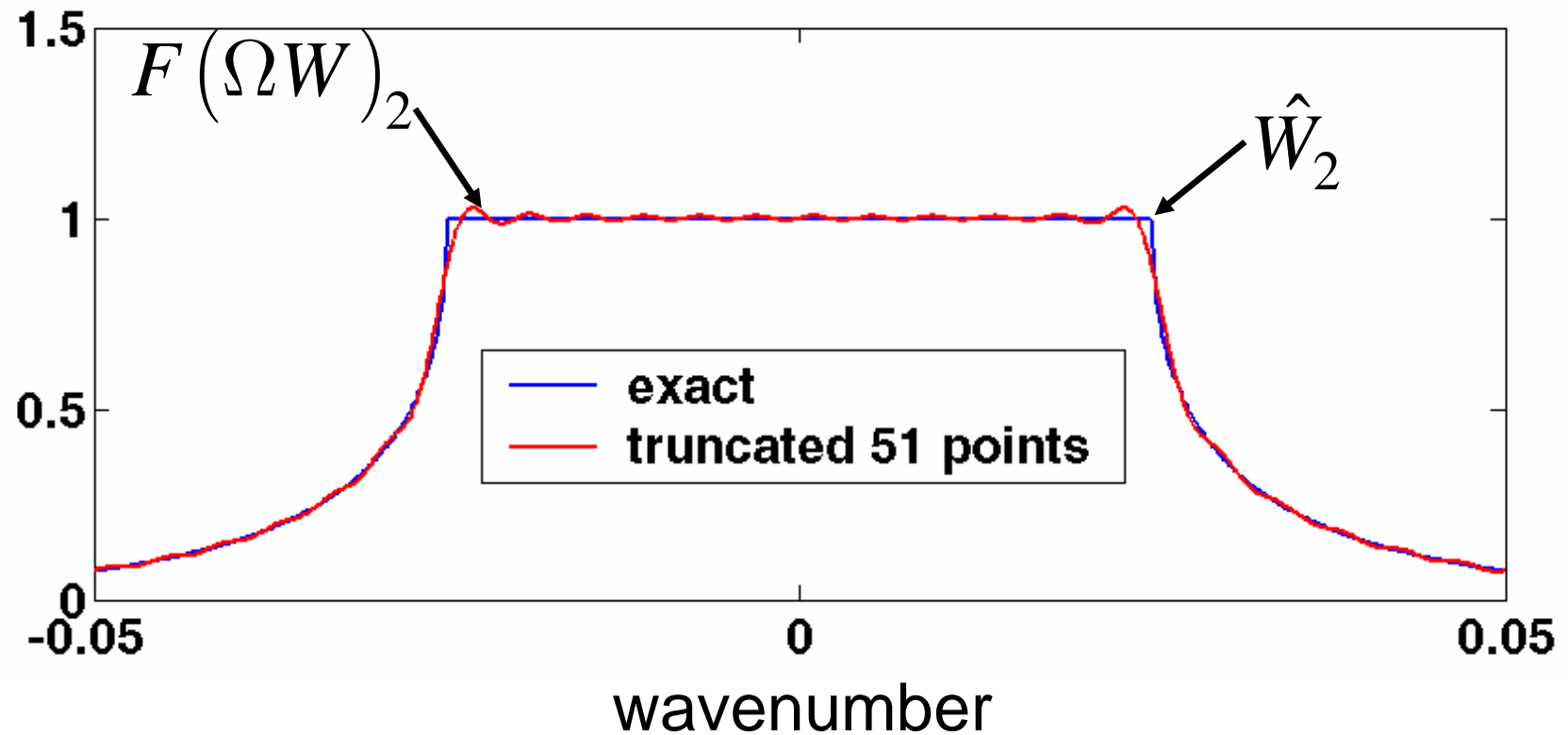
Wavefield Extrapolators

In the space-frequency domain



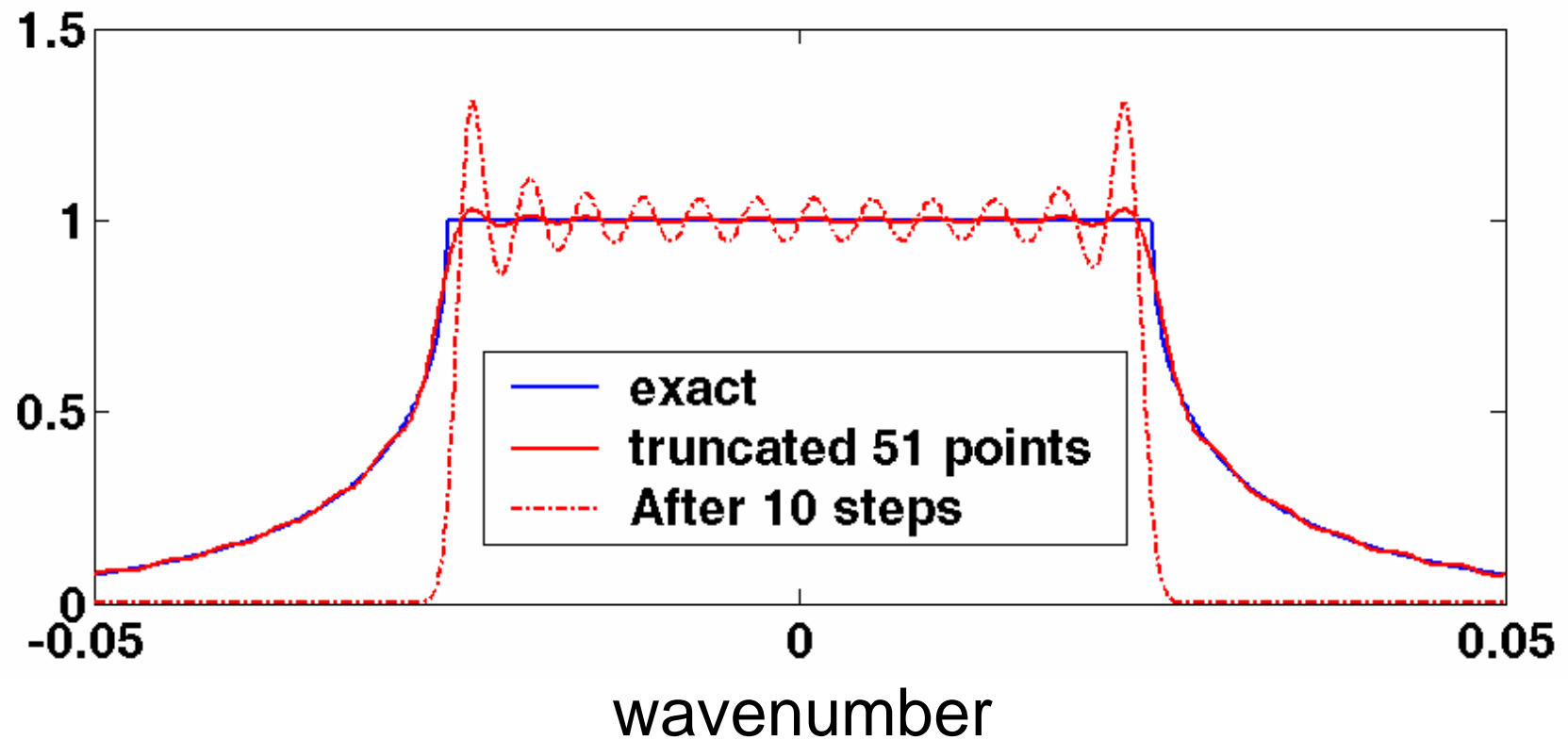
Wavefield Extrapolators

Back to the wavenumber domain



Wavefield Extrapolators

Back to the wavenumber domain



Stabilization by Wiener Filter

Two useful properties

$$\hat{W}_n(k_T, z, \omega) = \hat{W}_n\left(k_T, \frac{z}{2}, \omega\right) \hat{W}_n\left(k_T, \frac{z}{2}, \omega\right)$$

Product of two half-steps make a whole step.

$$\hat{W}_n^{-1}(k_T, z, \omega) = \hat{W}_n^*(k_T, z, \omega), \quad k^2 > k_x^2$$

The inverse is equal to the conjugate
in the wavelike region.

Stabilization by Wiener Filter

A windowed forward operator for a half-step

$$\tilde{W}_n(z/2) = \Omega W_n(z/2)$$

Solve by least squares

$$\tilde{W}_n(z/2) \bullet WI_n = F^{-1} \left[\left| \hat{W}_n(z/2) \right|^\eta \right]$$

$$0 \leq \eta \leq 2$$

Stabilization by Wiener Filter

WI_n is a band-limited inverse for $\tilde{W}_n(z/2)$
Both have compact support

Form the FOCI™ approximate operator by

$$W_{nF}(z) = WI_n^* \bullet \tilde{W}_n(z/2) \approx W_n(z)$$

FOCI™ is an acronym for

Forward Operator with Conjugate Inverse.

Linear System to Solve

$$\begin{bmatrix}
 \tilde{W}_{2,0} & \tilde{W}_{2,1} & \cdots & \tilde{W}_{2,p} & 0 & \cdots \\
 \tilde{W}_{2,1} & \tilde{W}_{2,0} & \tilde{W}_{2,1} & \cdots & 0 & \\
 \vdots & \tilde{W}_{2,1} & \tilde{W}_{2,0} & \ddots & \tilde{W}_{2,p} & \\
 \tilde{W}_{2,p} & \vdots & \tilde{W}_{2,1} & \ddots & \vdots & \\
 0 & \tilde{W}_{2,p} & \cdots & \ddots & \ddots & \tilde{W}_{2,1} \\
 \vdots & & \ddots & & \tilde{W}_{2,0} & \\
 0 & & & & \vdots &
 \end{bmatrix}
 \begin{bmatrix}
 WI_{2,0} \\
 WI_{2,1} \\
 \\ \\ \\
 WI_{2,m}
 \end{bmatrix}
 =
 \begin{bmatrix}
 D_{2,0} \\
 D_{2,1} \\
 D_{2,2} \\
 \vdots \\
 D_{2,m+p}
 \end{bmatrix}$$

Properties of FOCl operator

Let

$$n_{inv} = \text{length}(WI_n) \quad n_{for} = \text{length}(\tilde{W}_n(z/2))$$

Then

$$\text{length}(W_{nF}(z)) = n_{op} = n_{for} + n_{inv} - 1$$

Properties of FOCl operator

n_{for} determines phase accuracy.

n_{inv} determines stability.

Empirical observation:

$$n_{inv} \approx 1.5n_{for}$$

Properties of FOCI operator

Amount of evanescent filtering is inversely related to stability

$$\eta = \begin{cases} 0 \cdots \text{no evanescent filtering (} \sim 1000 \text{ steps)} \\ 1 \cdots \text{half evanescent filtering (} \sim 100 \text{ steps)} \\ 2 \cdots \text{full evanescent filtering (} \sim 50 \text{ steps)} \end{cases}$$

Operator tables

Since the operator is purely numerical, migration proceeds by construction of operator tables.

| | |
|------------------------|--------------------------------|
| k_{\min} | $W_{nF}(k_{\min})$ |
| $k_{\min} + \Delta k$ | $W_{nF}(k_{\min} + \Delta k)$ |
| $k_{\min} + 2\Delta k$ | $W_{nF}(k_{\min} + 2\Delta k)$ |
| ... | ... |
| k_{\max} | $W_{nF}(k_{\max})$ |

$$k_{\min} = \frac{\omega_{\min}}{v_{\max}} \quad \Delta k = \frac{\Delta\omega}{\text{mean}(v)} \quad k_{\max} = \frac{\omega_{\max}}{v_{\min}}$$

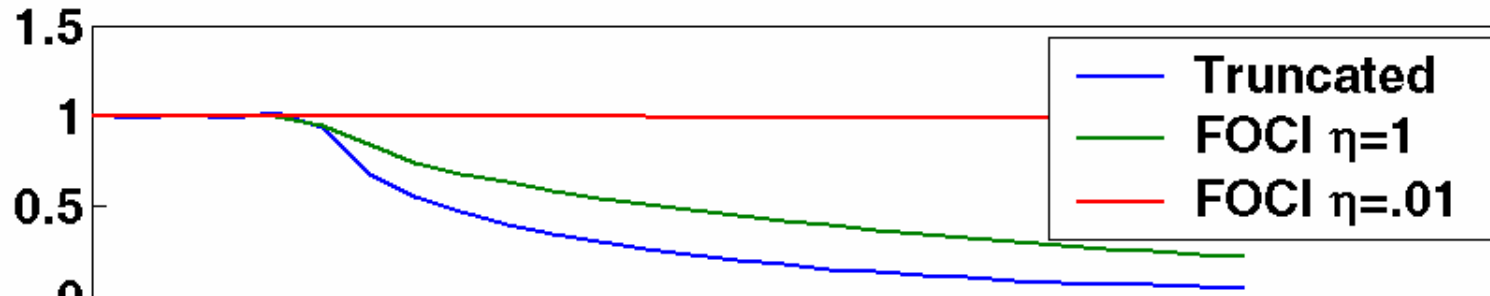
Operator tables

We construct two operator tables for small and large η . The small η table is used most of the time, with the large η being invoked only every n^{th} step.

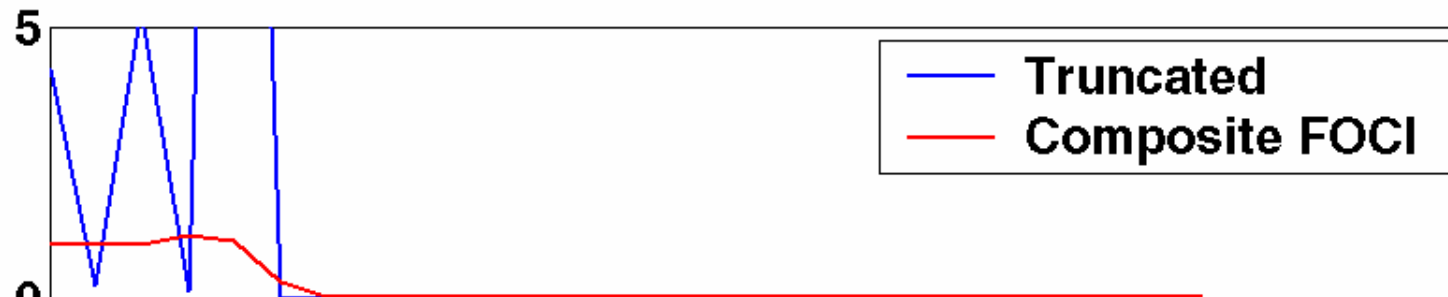
$$\eta = \begin{cases} 0 \cdots \text{no evanescent filtering (} \sim 1000 \text{ steps)} \\ 1 \cdots \text{half evanescent filtering (} \sim 100 \text{ steps)} \\ 2 \cdots \text{full evanescent filtering (} \sim 50 \text{ steps)} \end{cases}$$

Operator Design Example

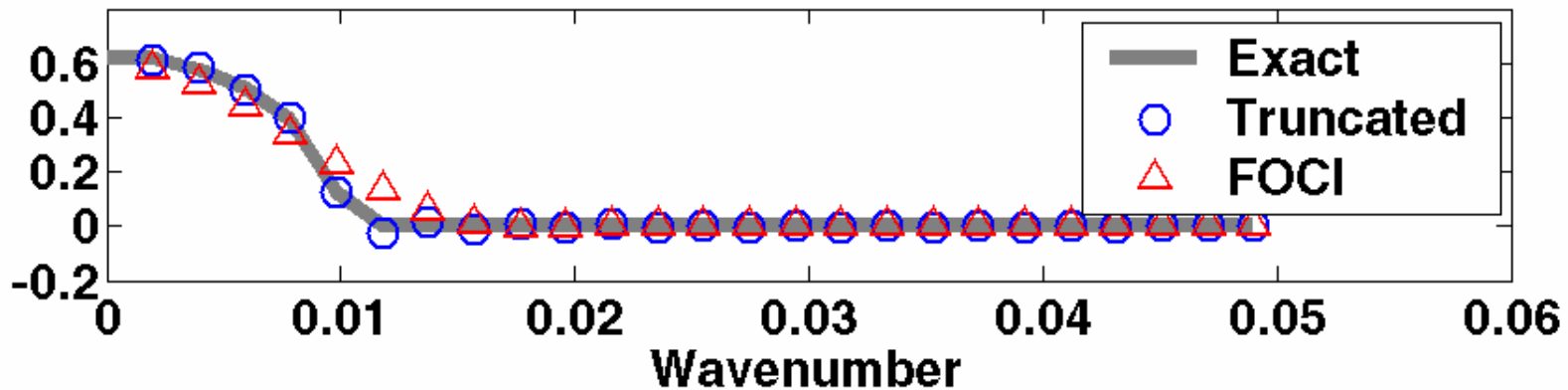
Amplitude spectra



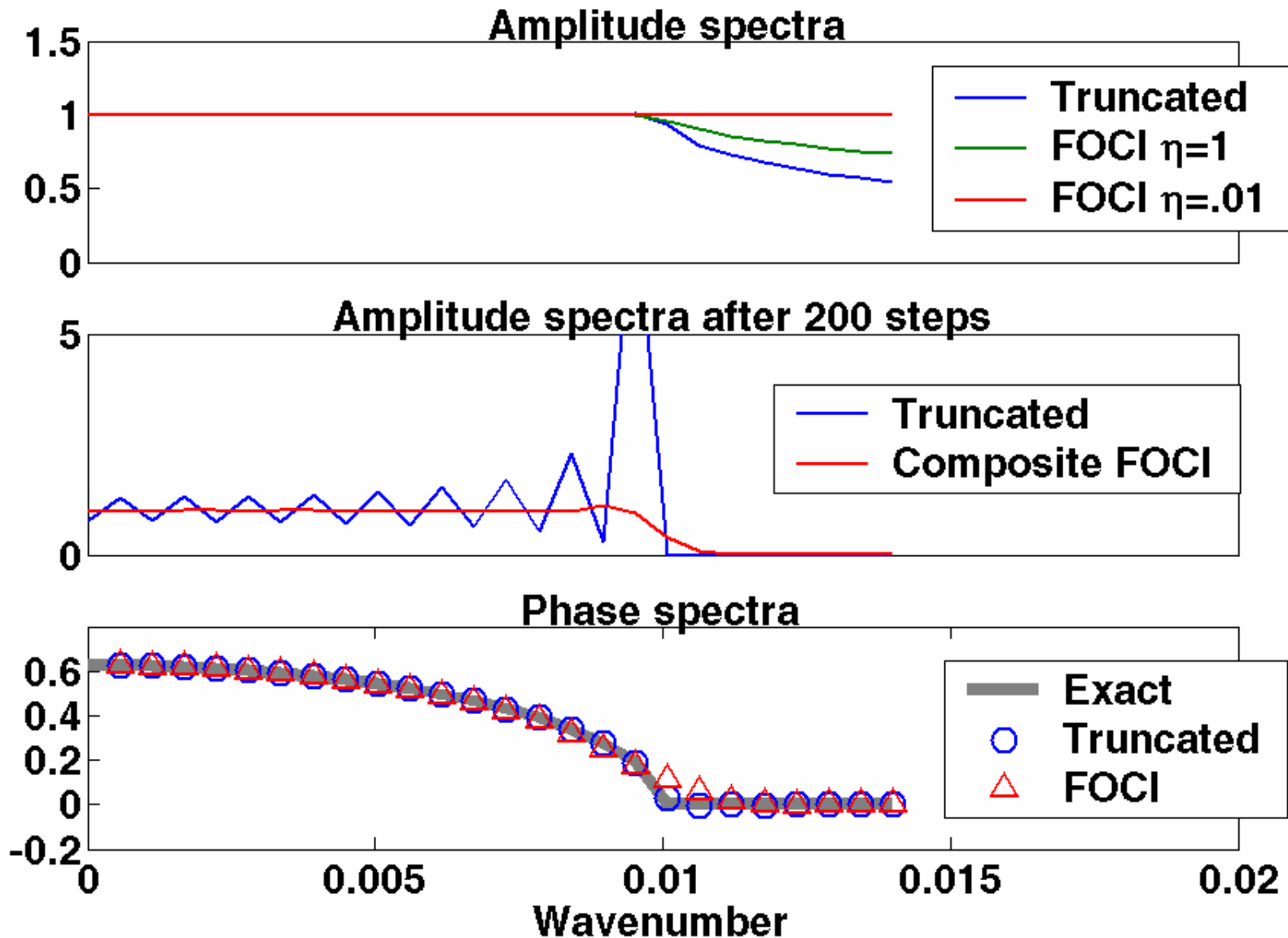
Amplitude spectra after 200 steps



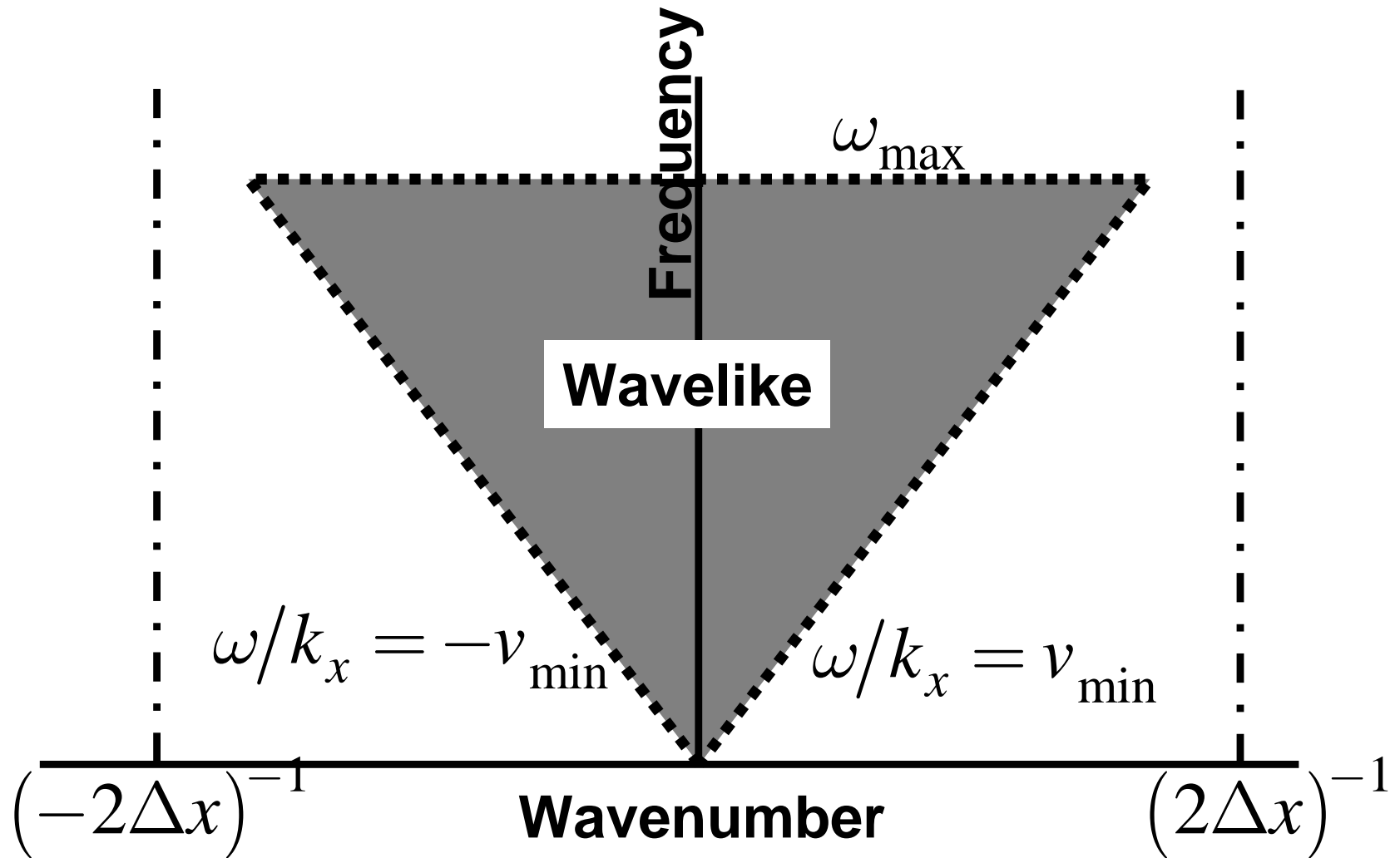
Phase spectra



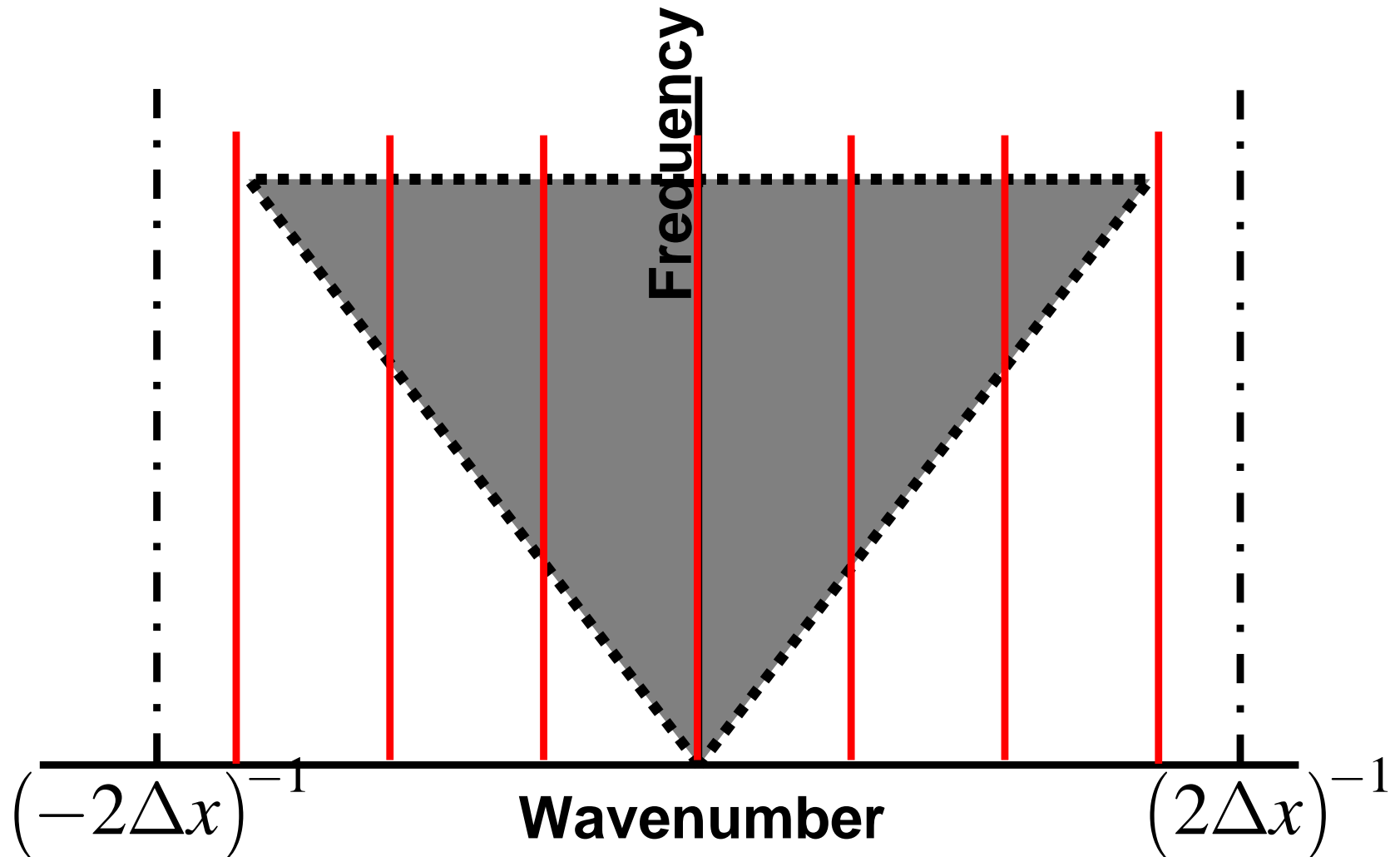
Improved Operator Design



Spatial Resampling

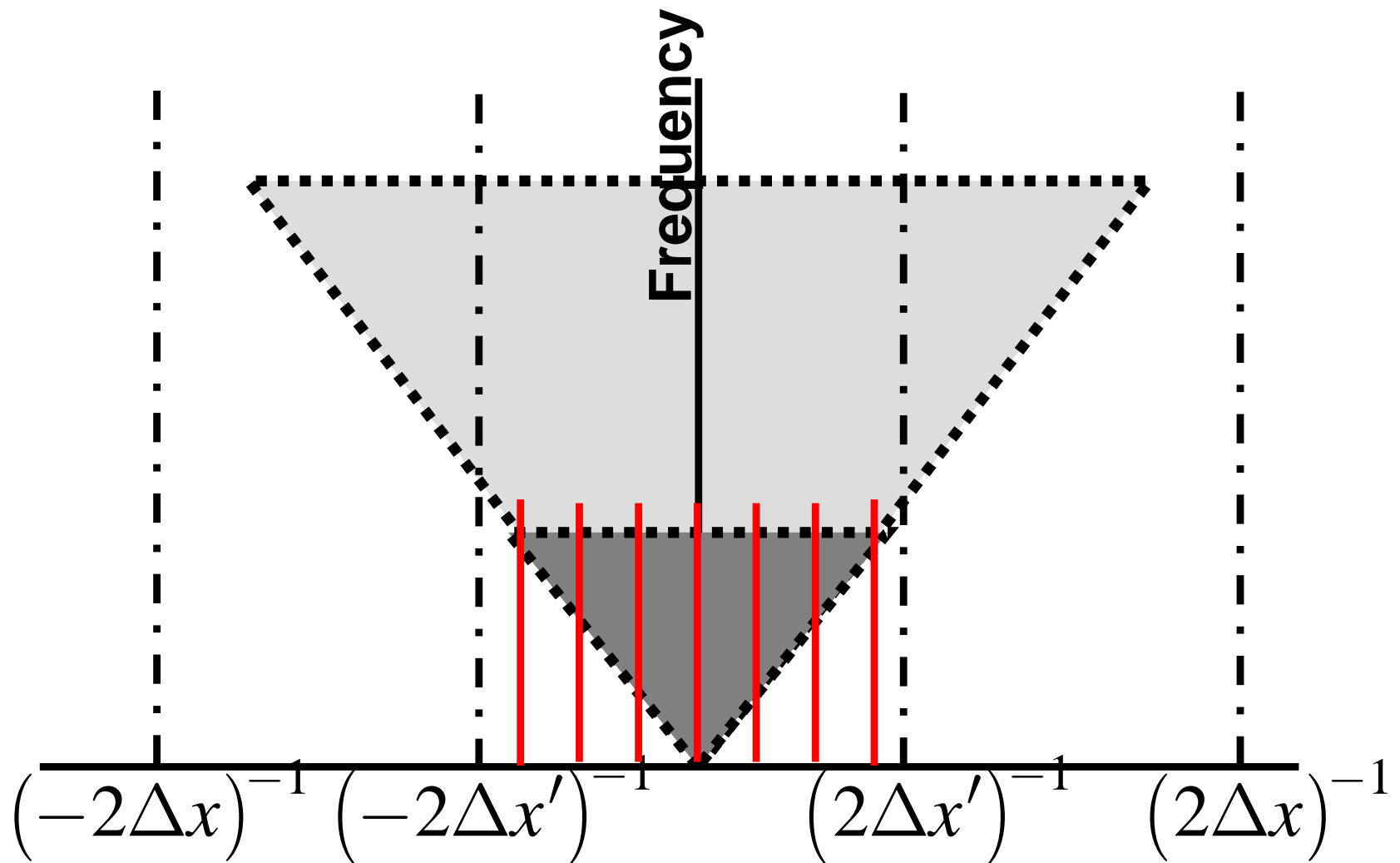


Spatial Resampling



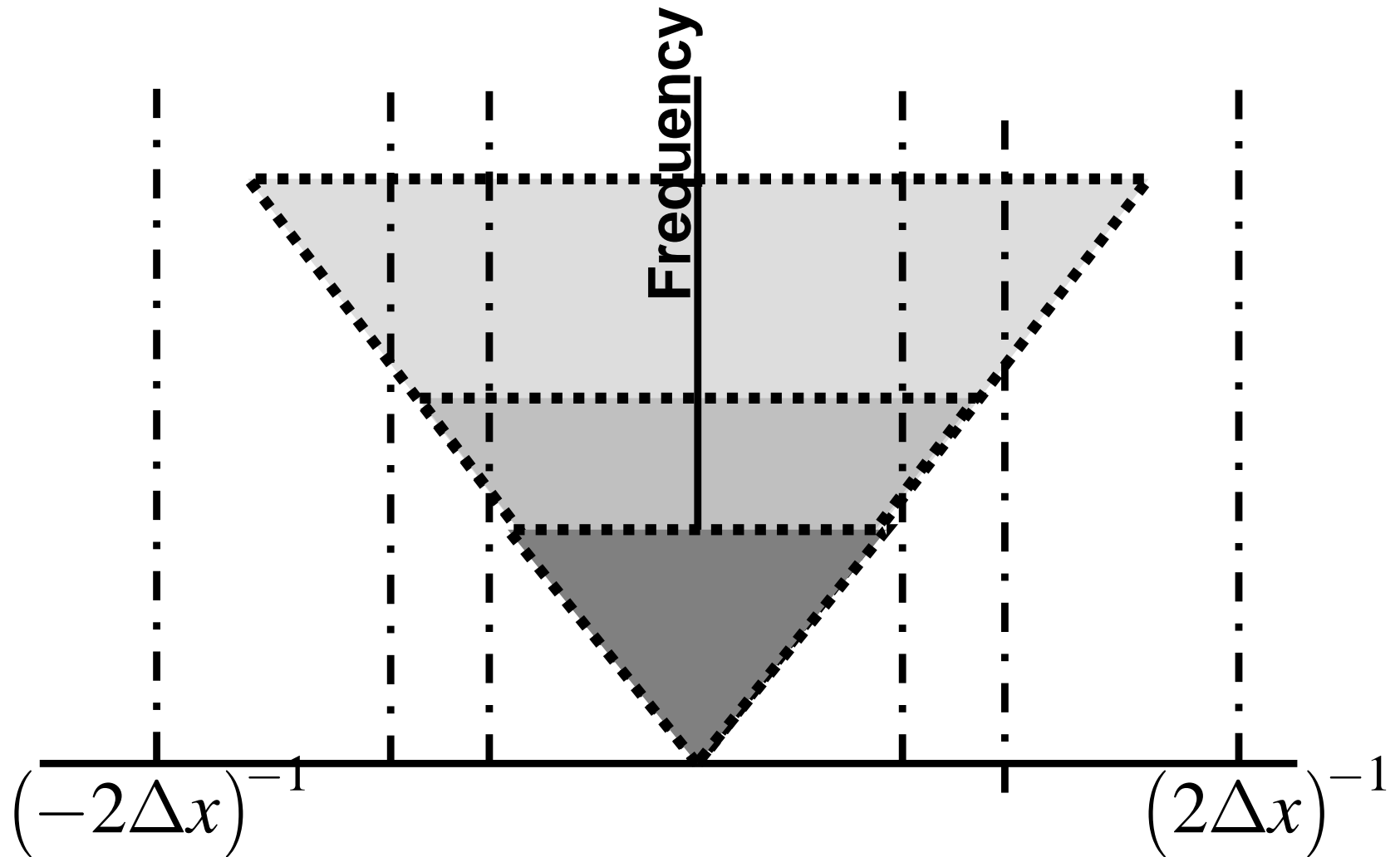
In red are the wavenumbers of a 7 point filter

Spatial Resampling



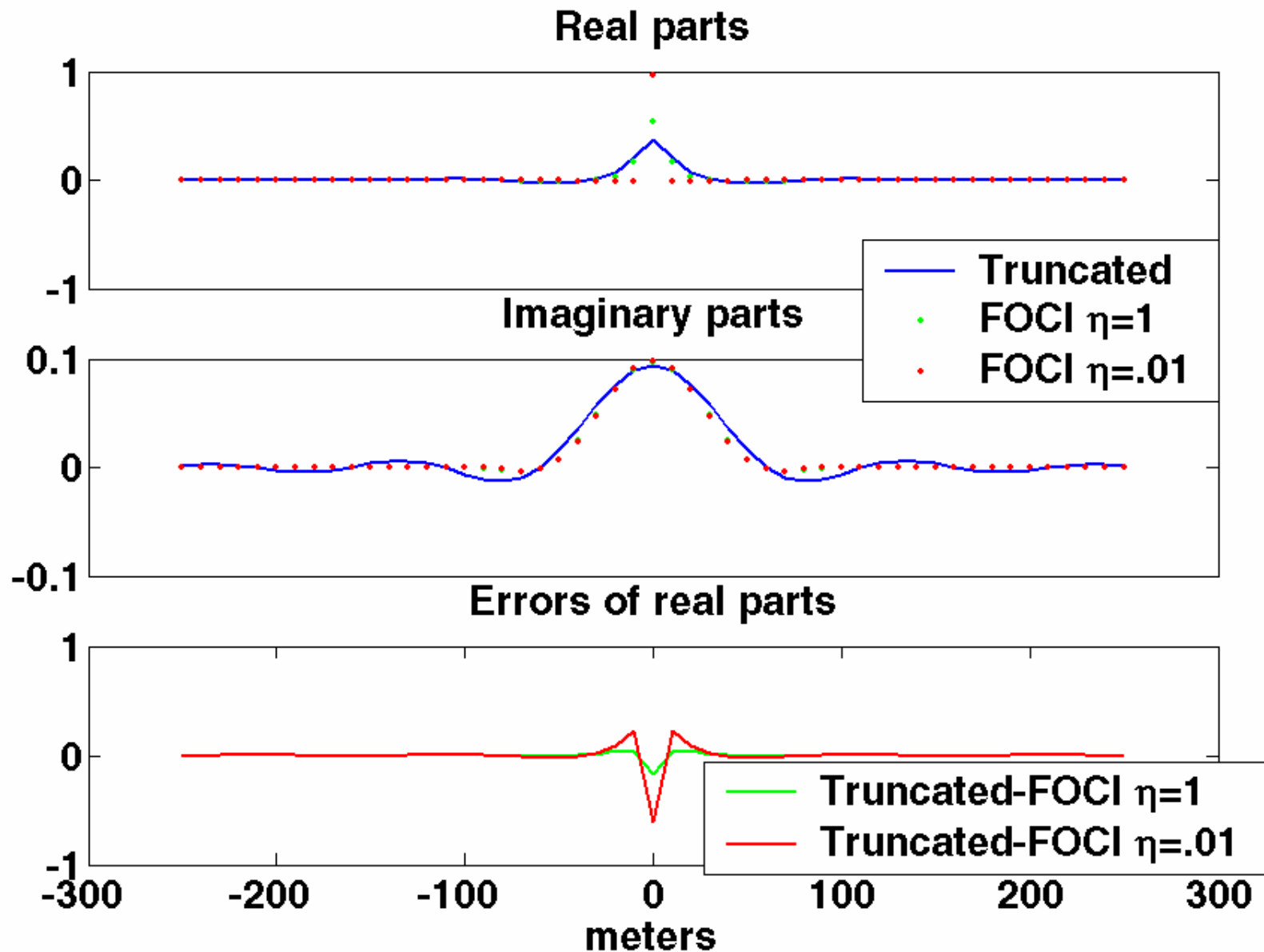
Downsampling for the lower frequencies uses the filter more effectively

Spatial Resampling

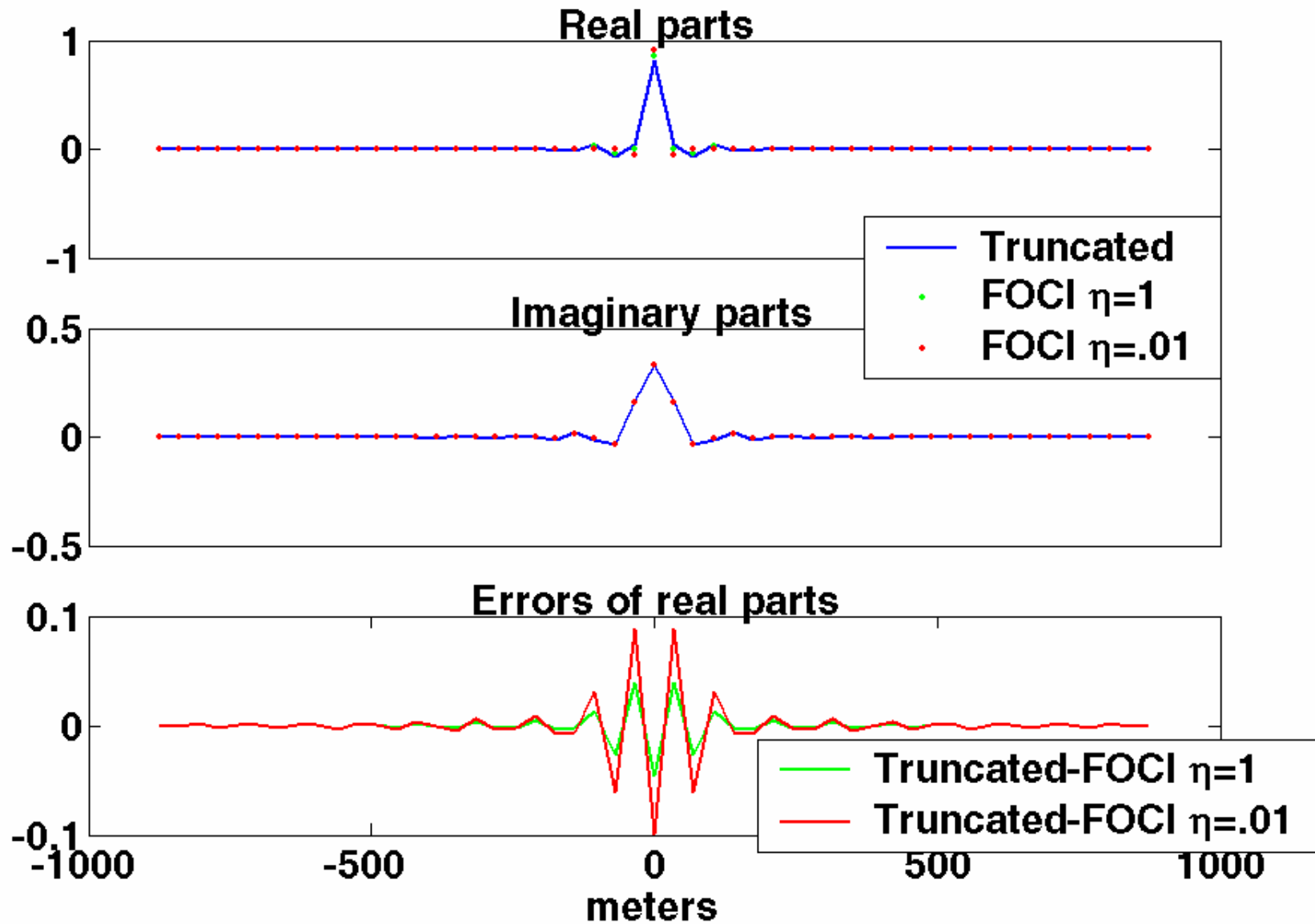


Spatial resampling is done in frequency “chunks”.

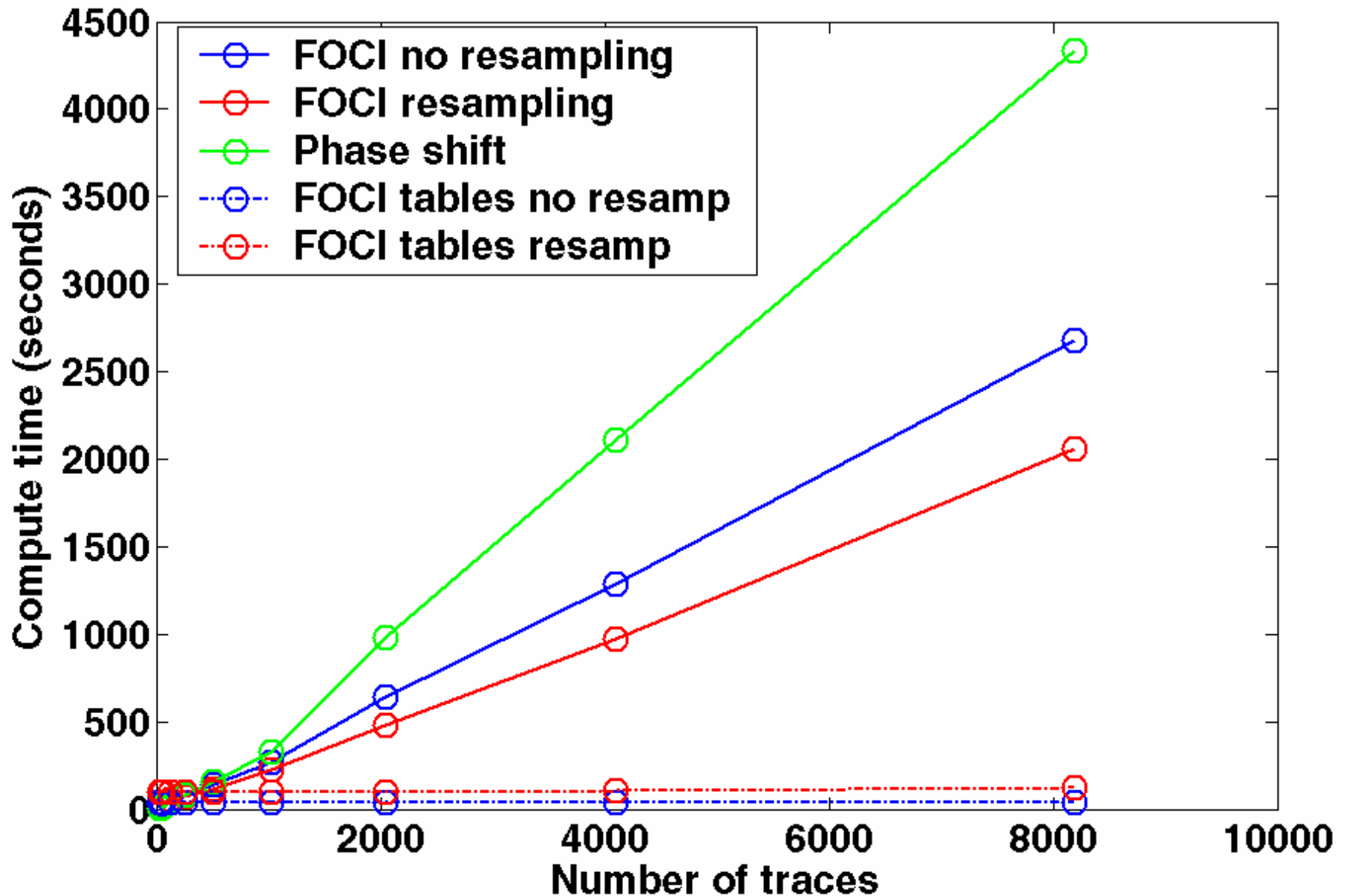
Operator in Space



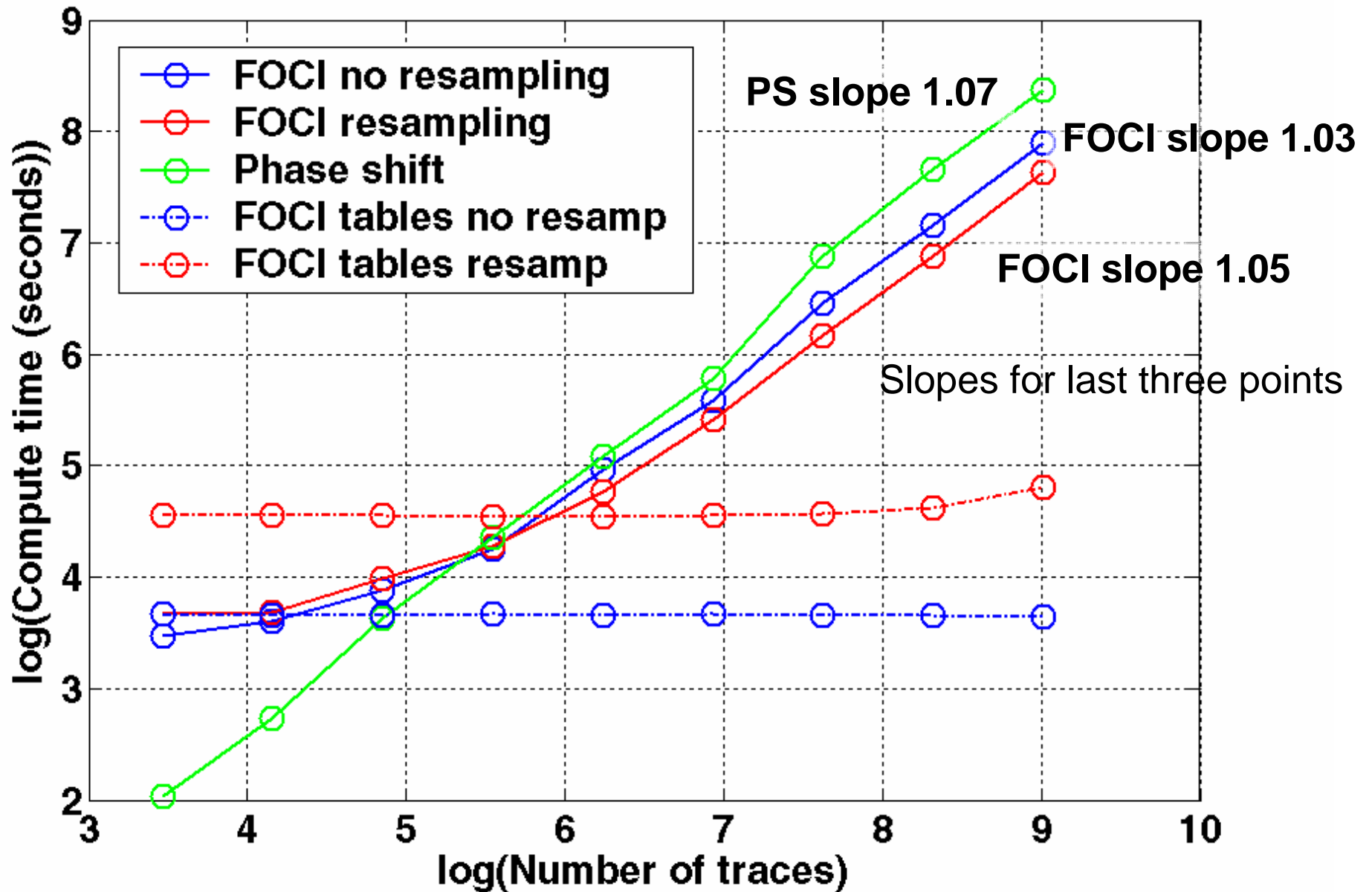
Improved Operator in Space



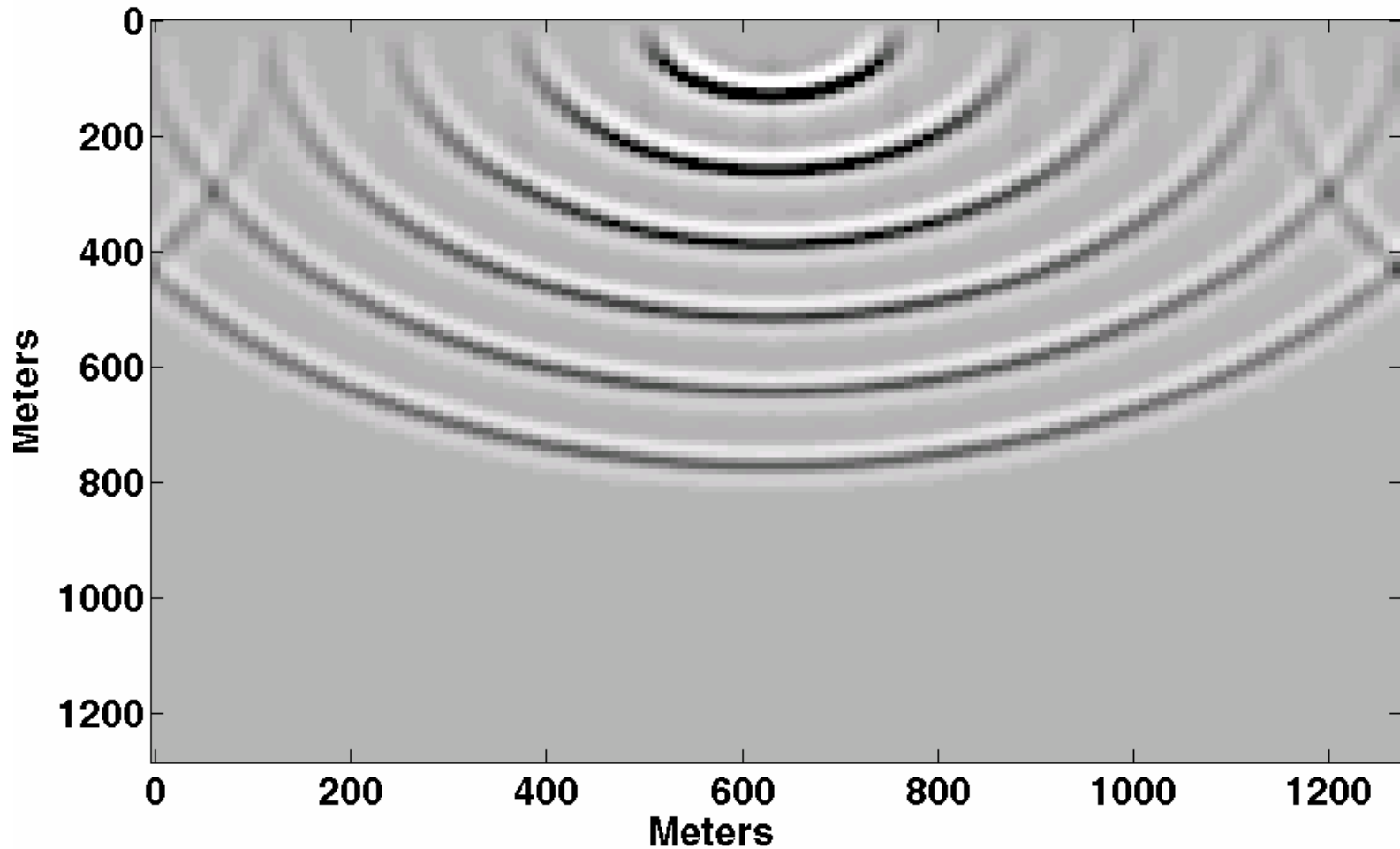
Run Time Experiment



Run Times log-log Scale

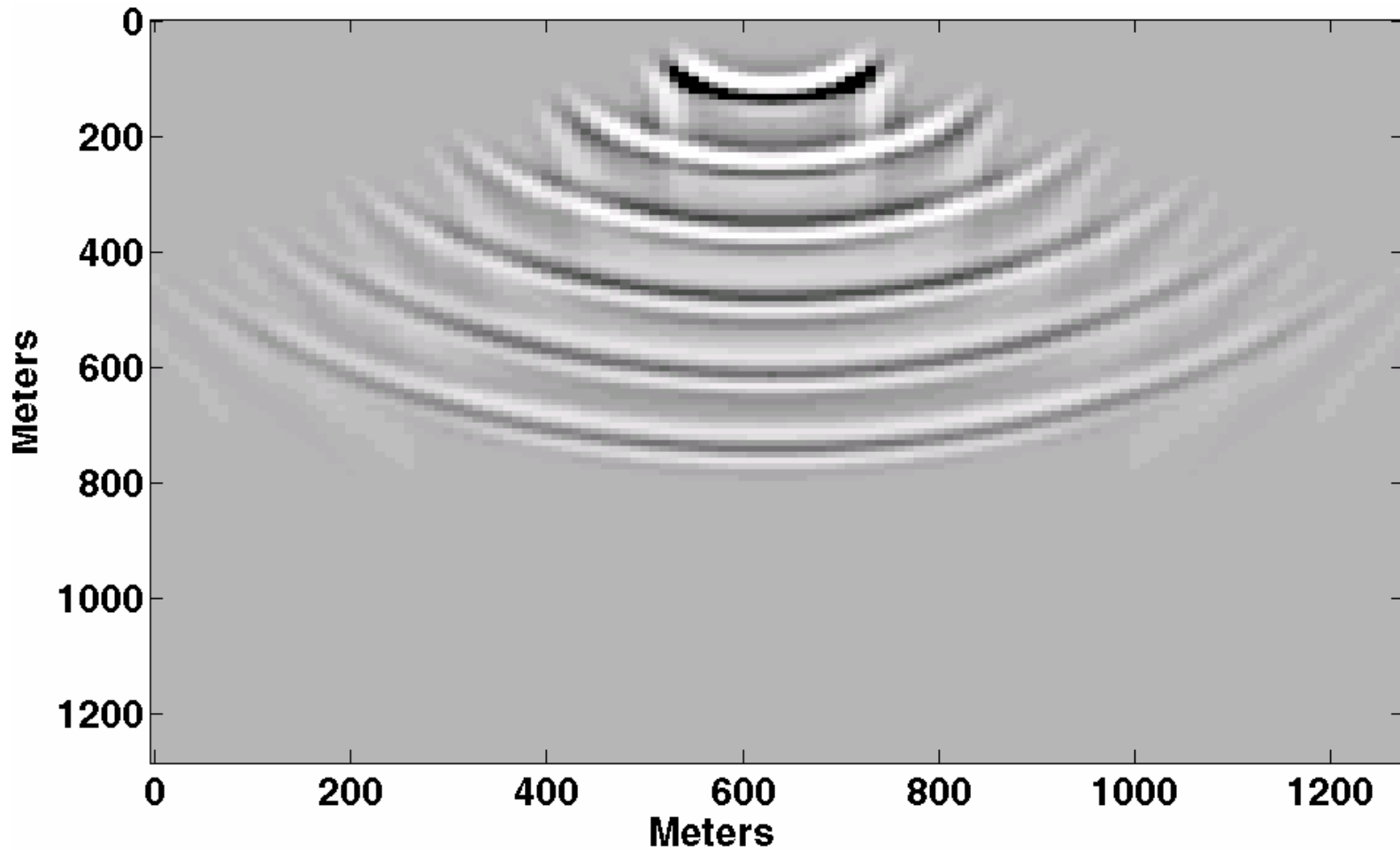


Phase Shift Impulse Response



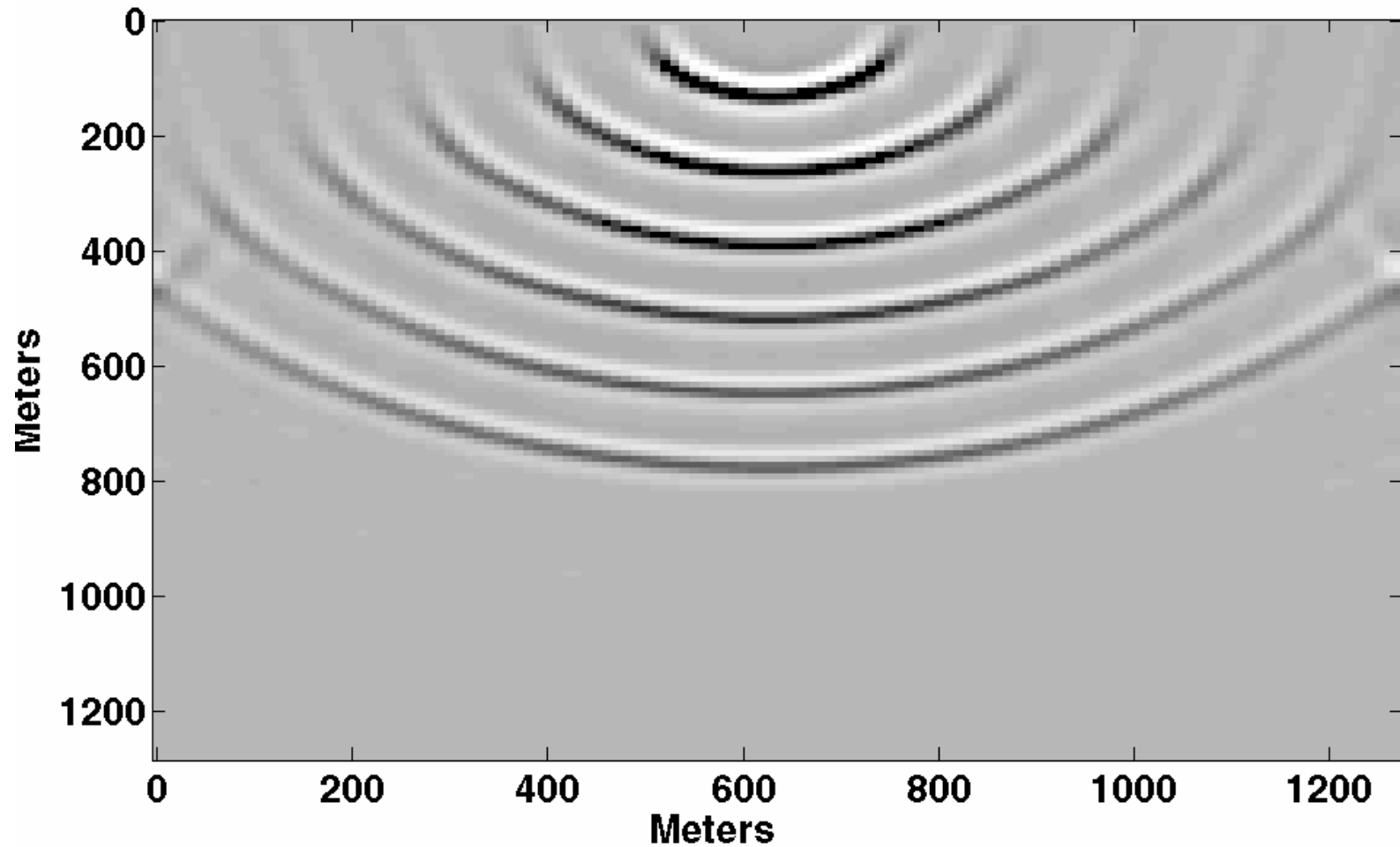
FOCI Impulse Response

nfor=7, ninv=15, (21 pt), no spatial resampling

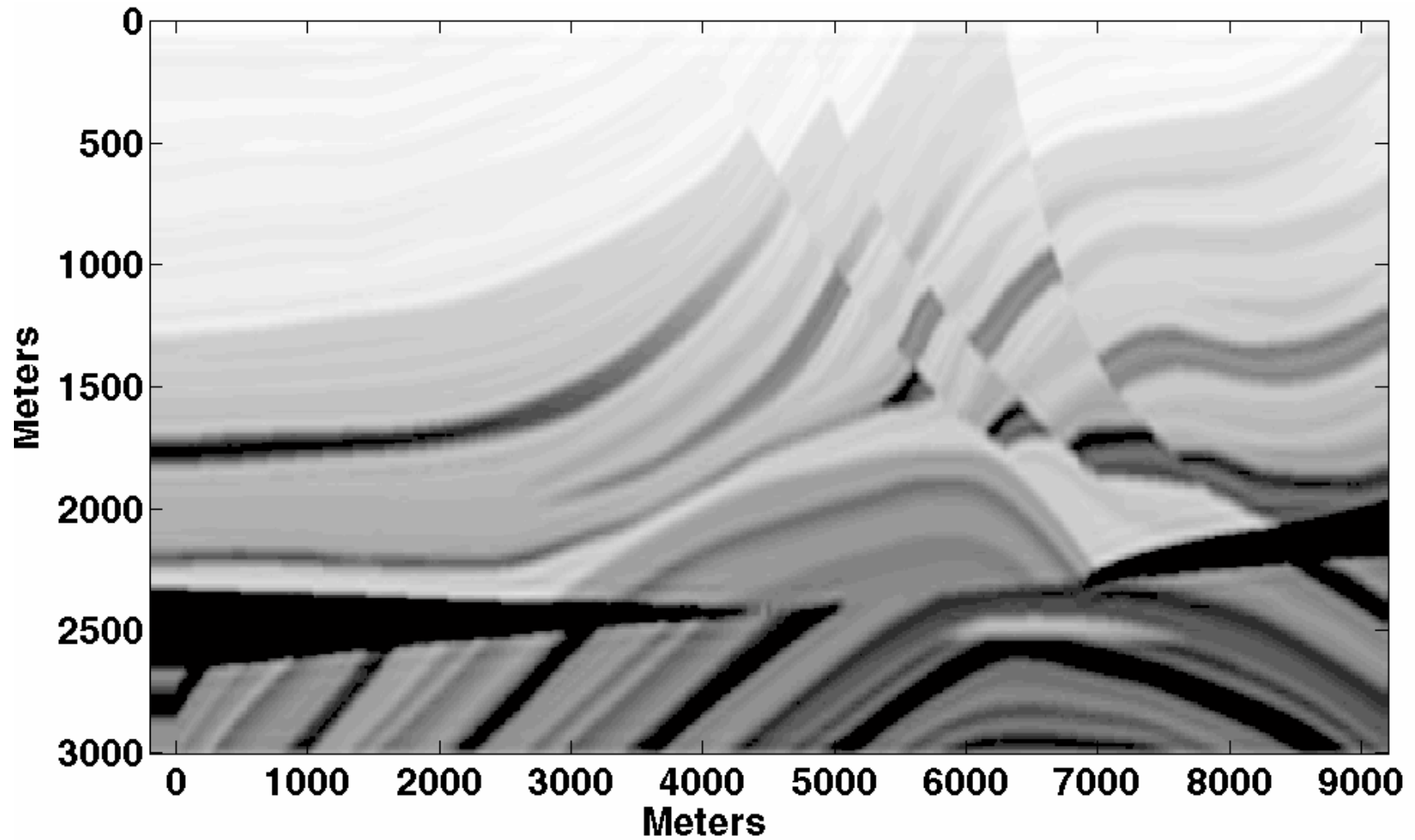


FOCI Impulse Response

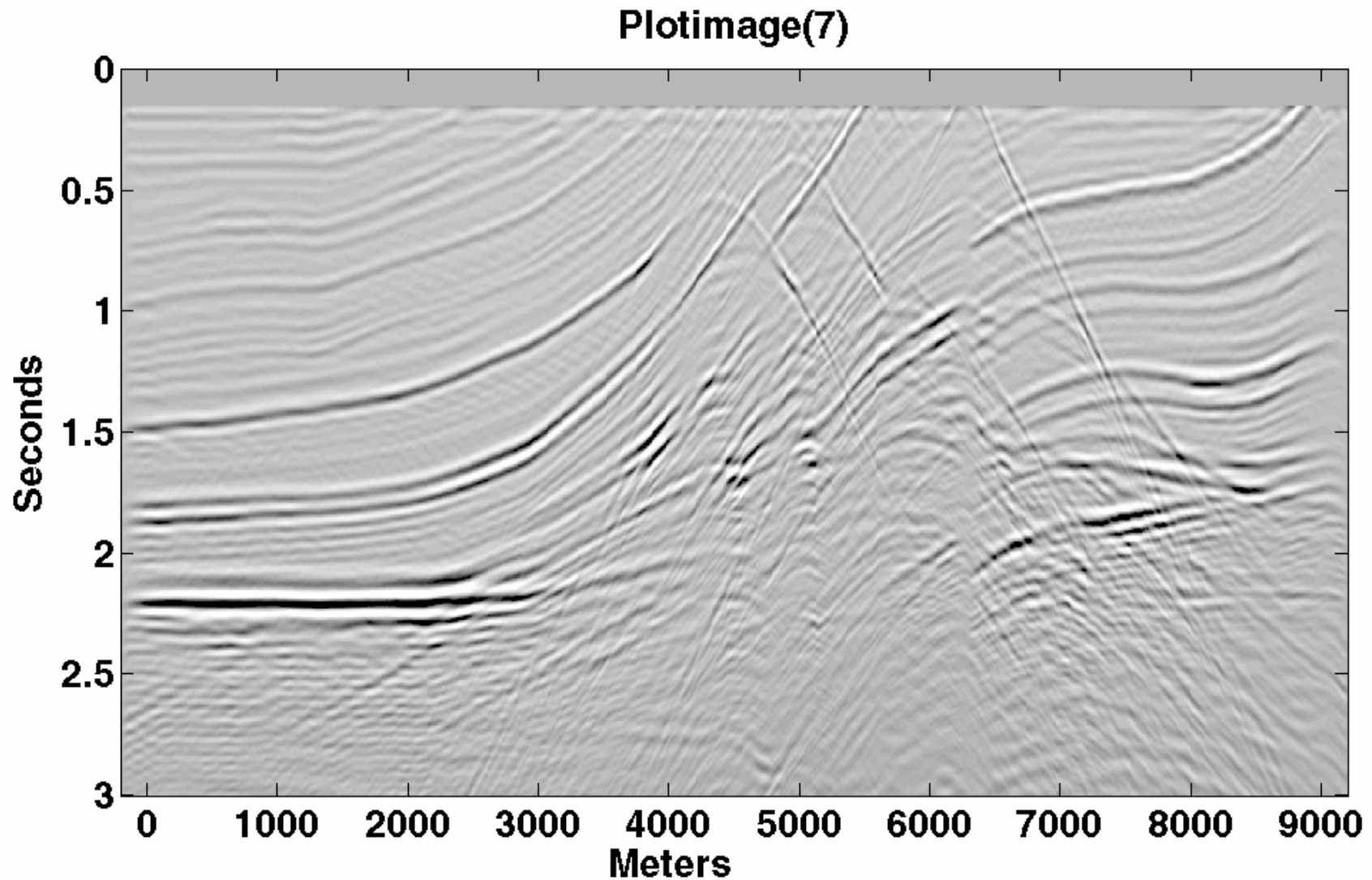
nfor=7, ninv=15, (21 pt), with spatial resampling



Marmousi Velocity Model

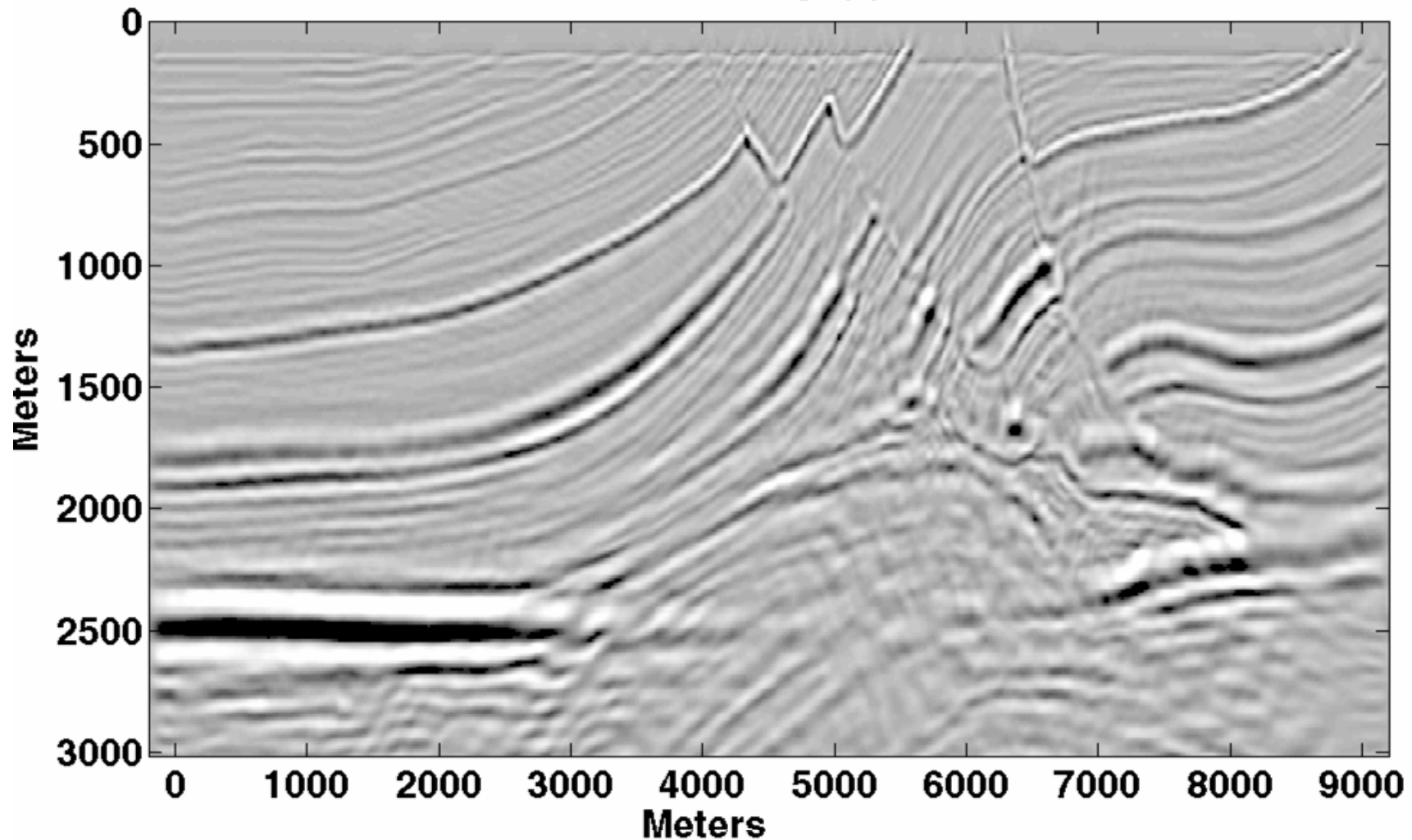


Exploding Reflector Seismogram



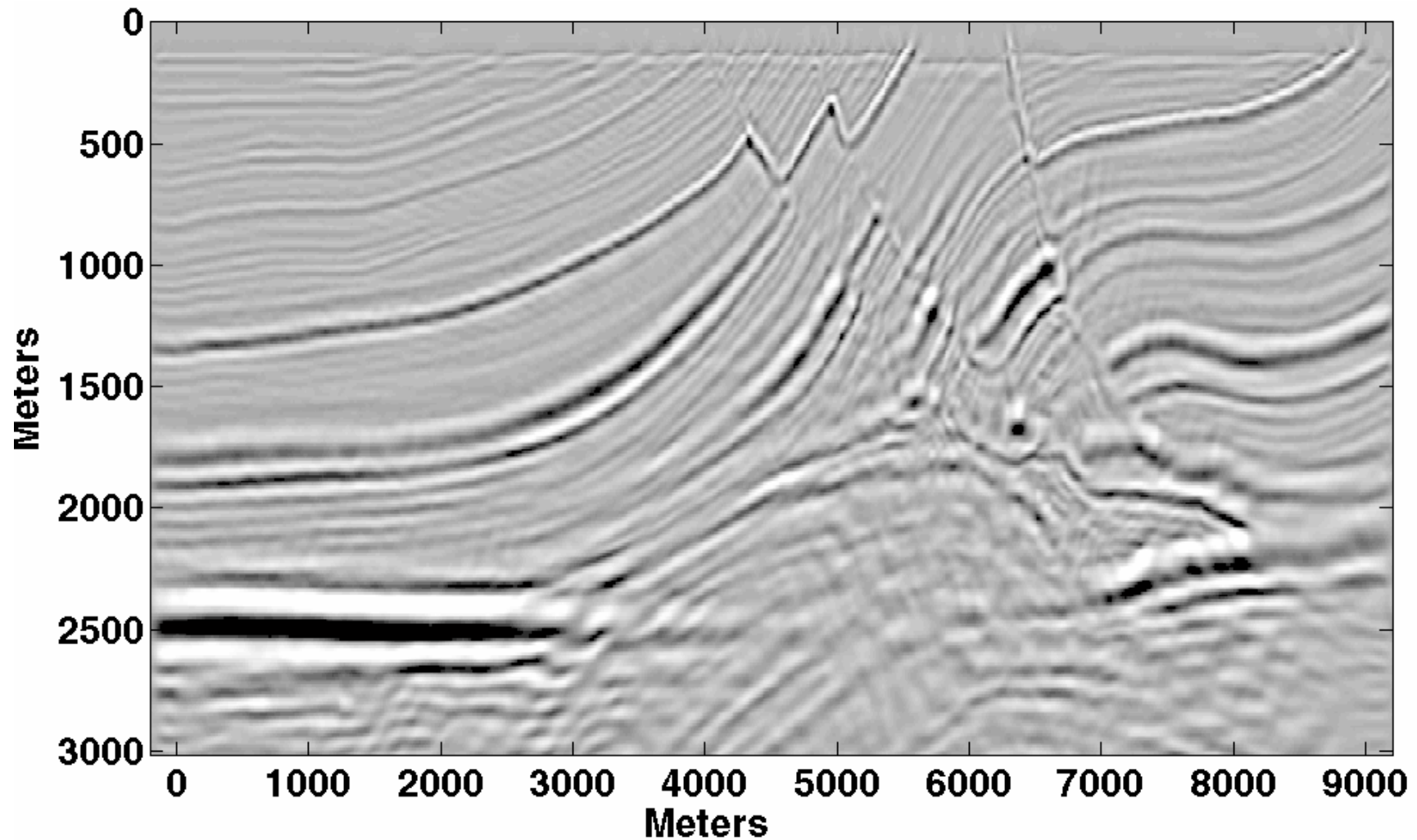
FOCI Post-Stack Migration

nfor=21, ninv=31, nwin=0



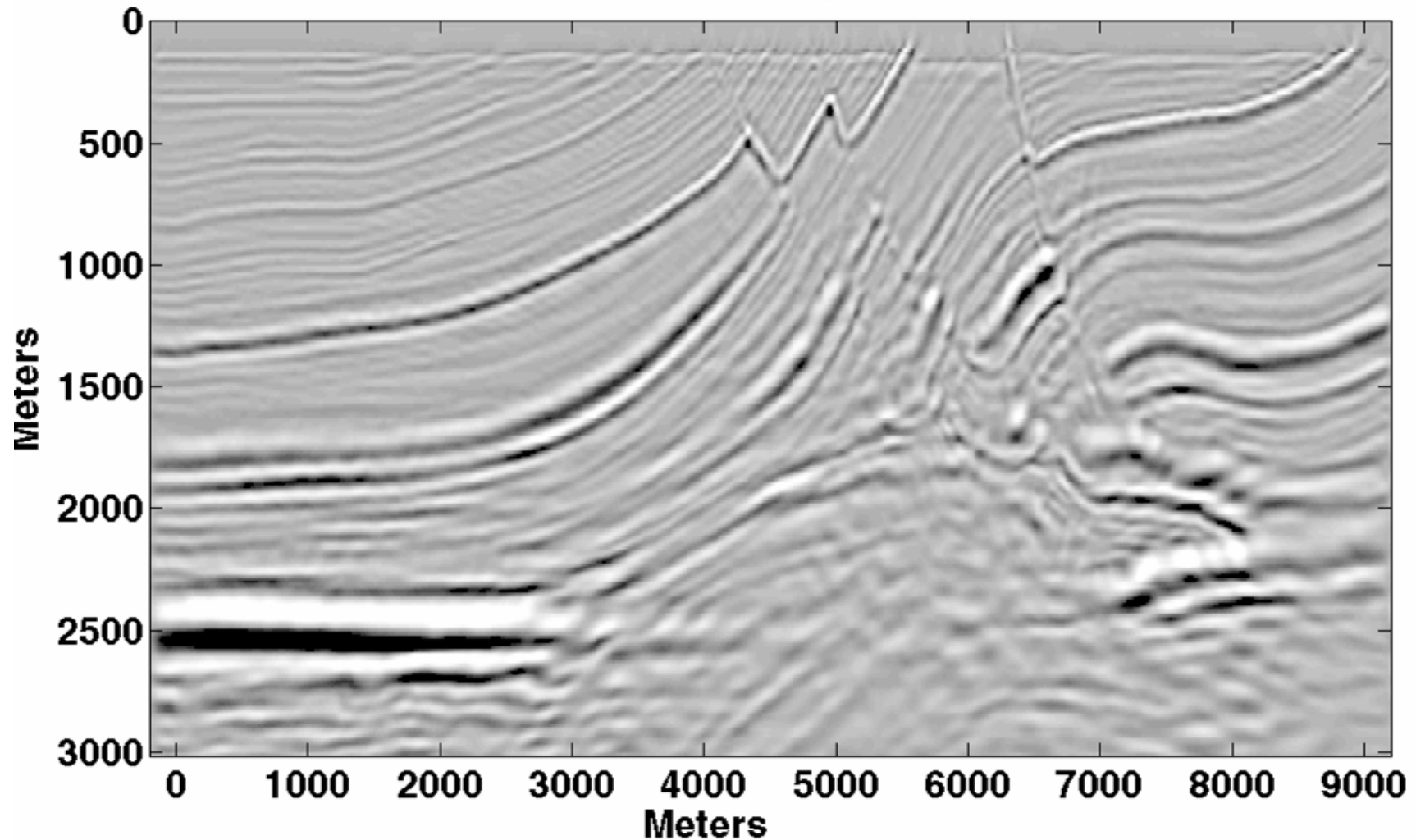
FOCI Post-Stack Migration

nfor=21, ninv=31, nwin=51



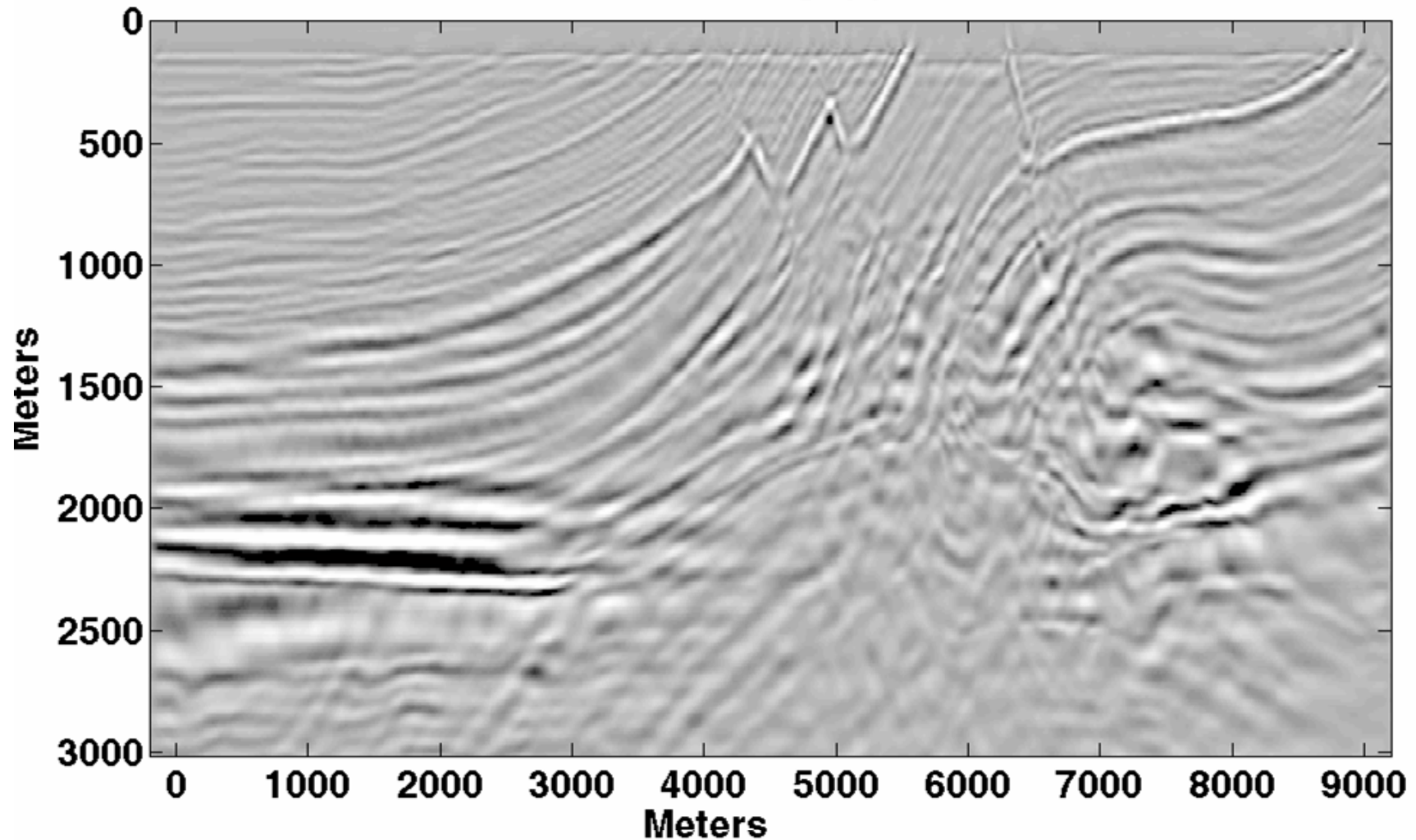
FOCI Post-Stack Migration

nfor=21, ninv=31, nwin=21



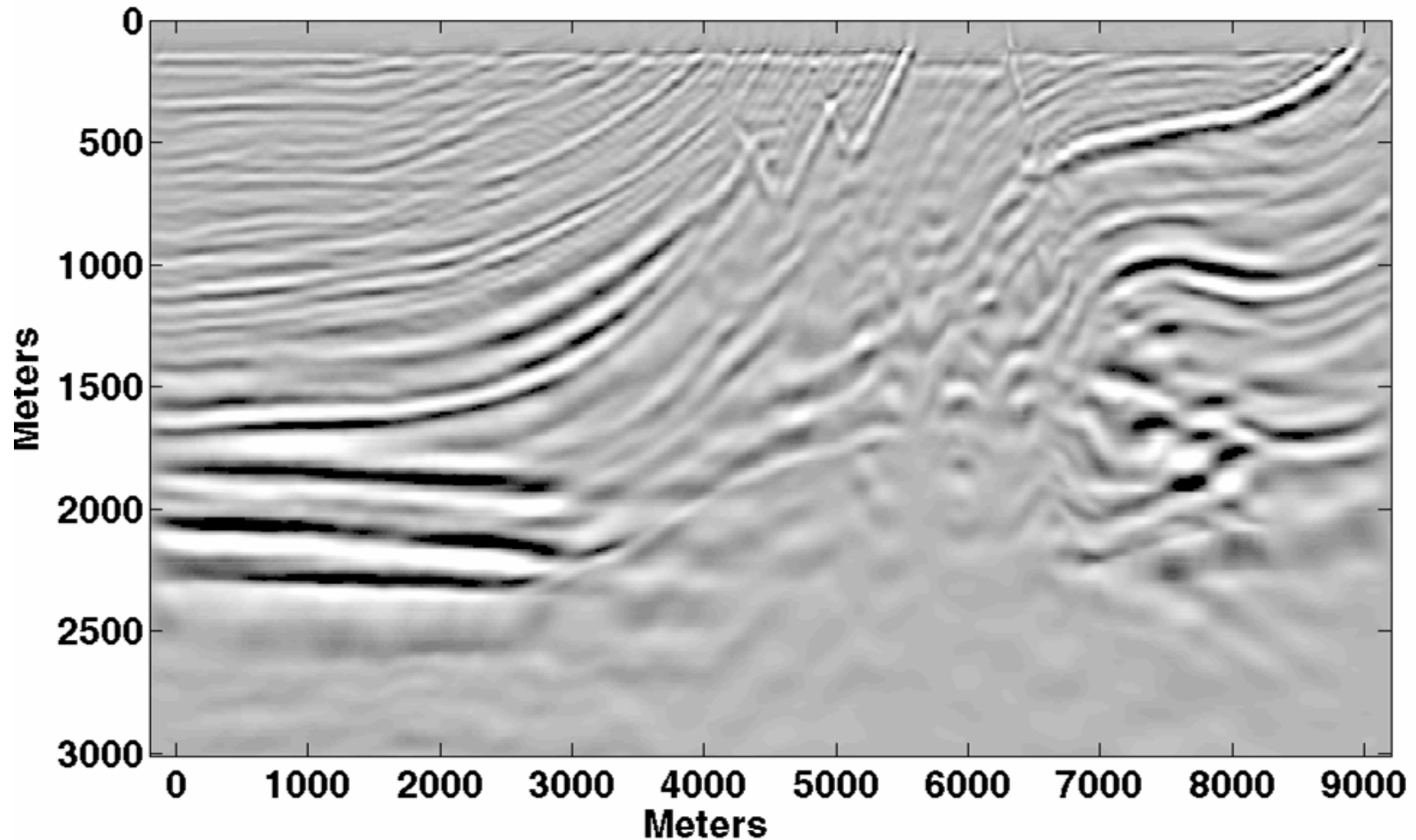
FOCI Post-Stack Migration

nfor=7, ninv=15, nwin=0

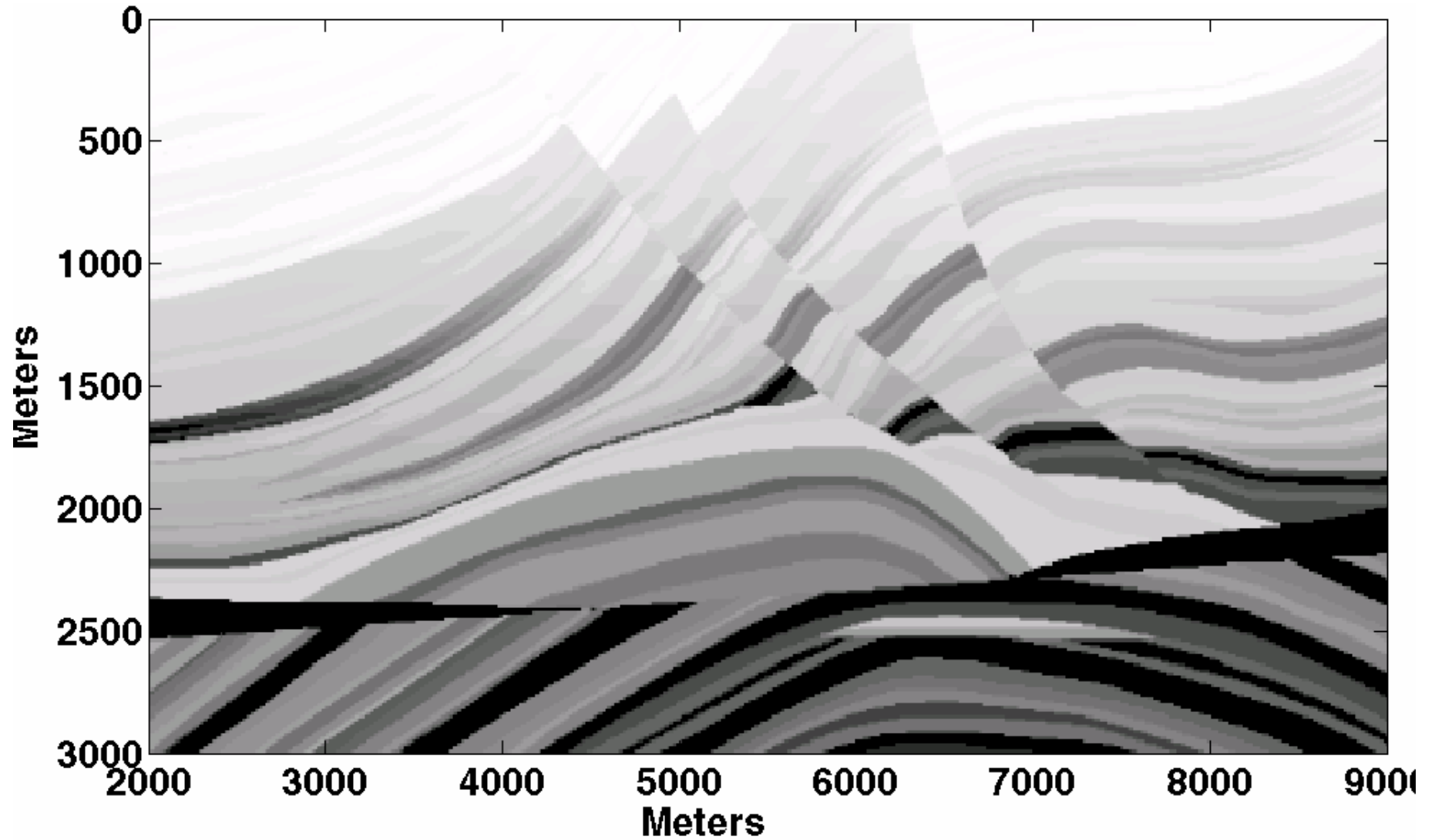


FOCI Post-Stack Migration

nfor=7, ninv=15, nwin=7

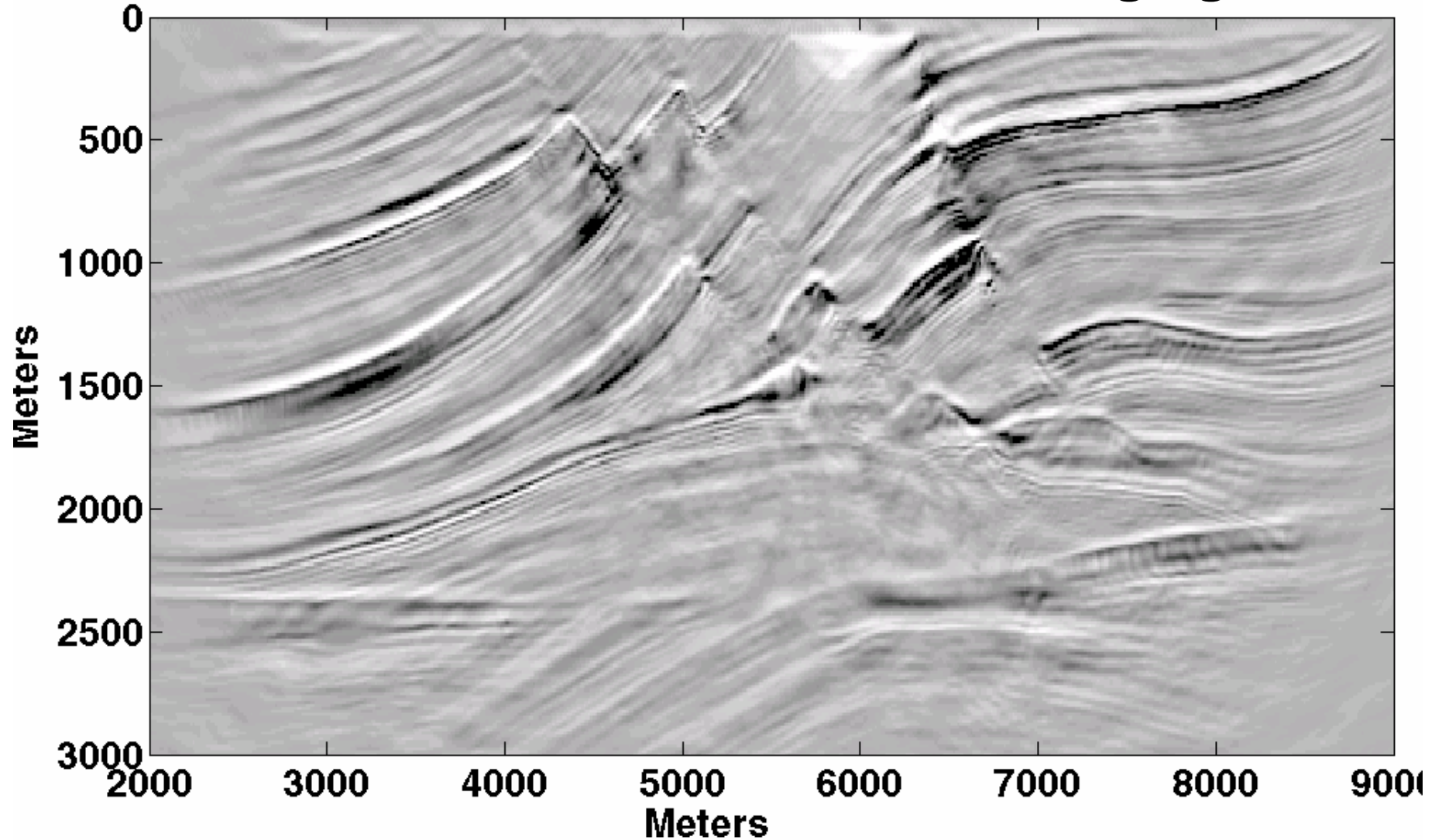


Marmousi Velocity Model



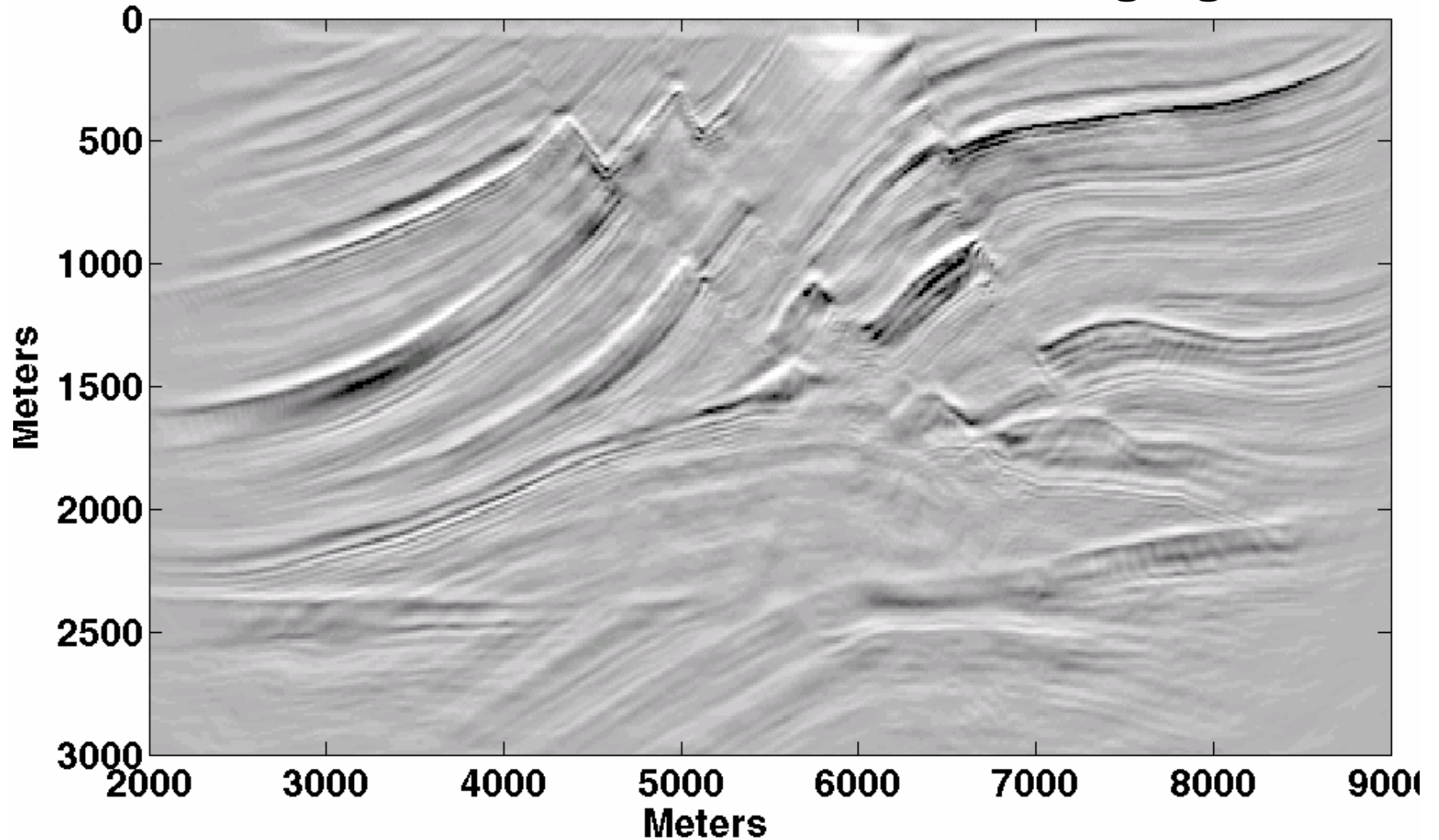
FOCI Pre-Stack Migration

nfor=21, ninv=31, nwin=0, deconvolution imaging condition



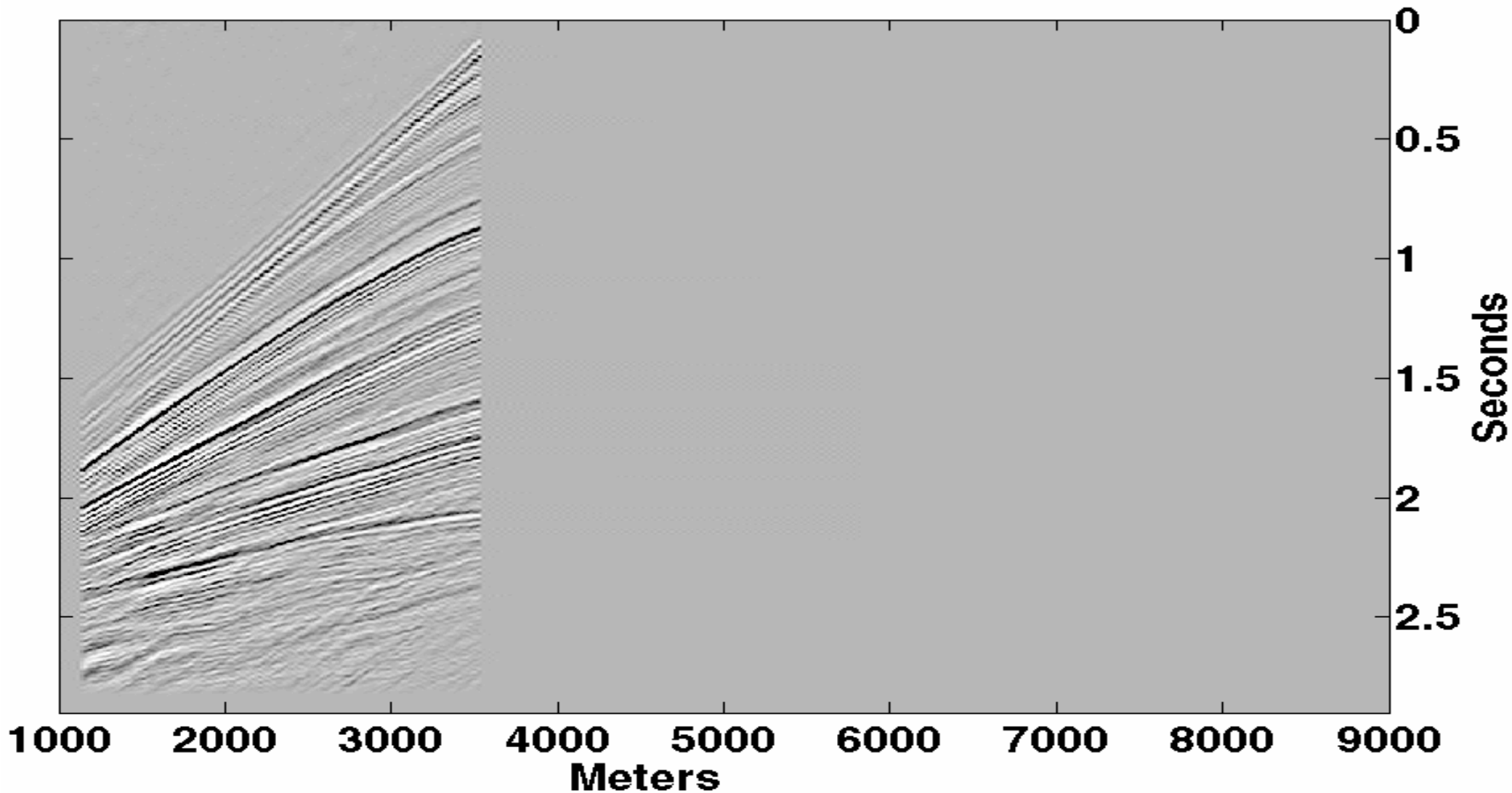
FOCI Pre-Stack Migration

nfor=21, ninv=31, nwin=0, deconvolution imaging condition



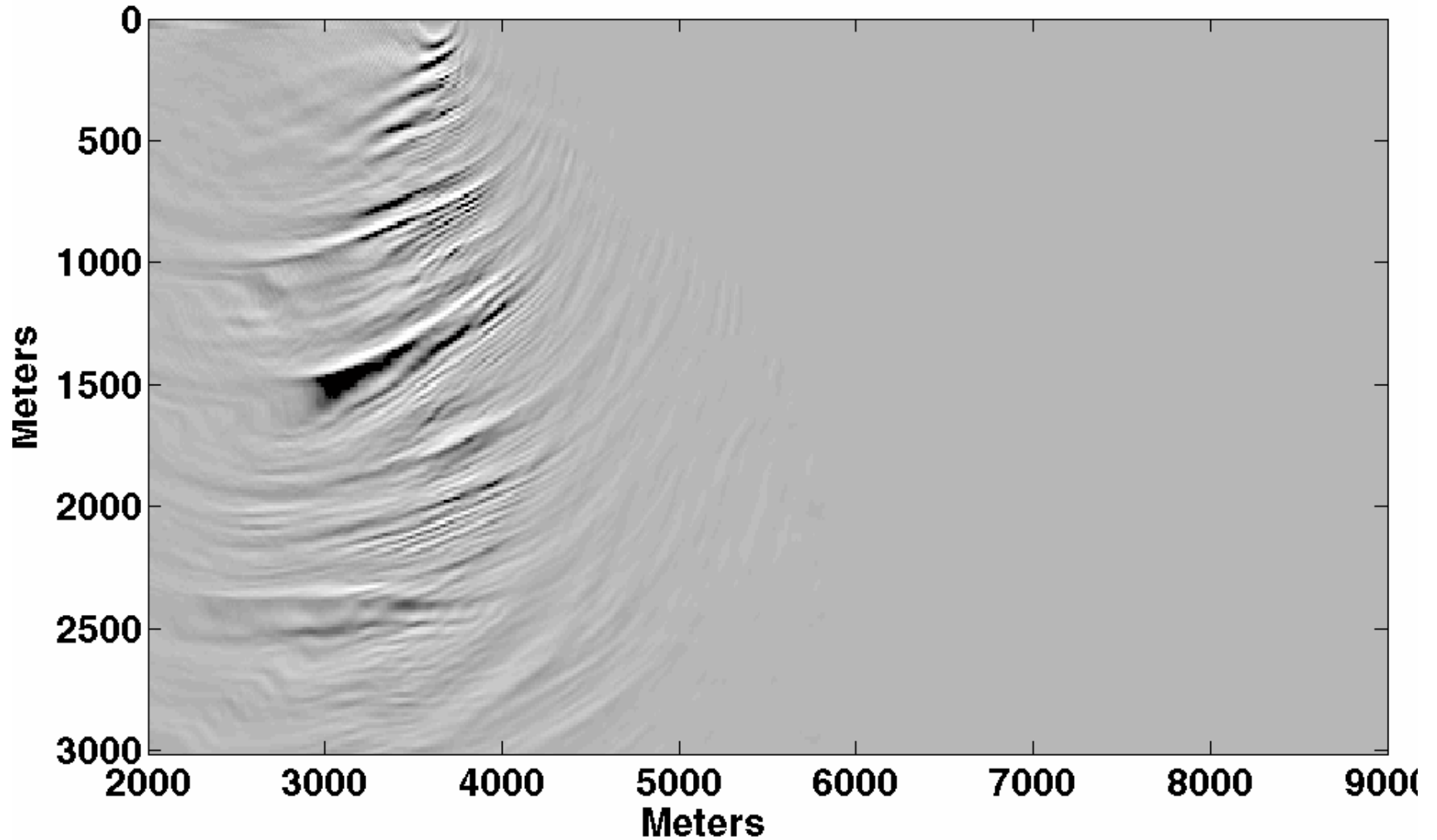
FOCI Pre-Stack Migration

Shot 30



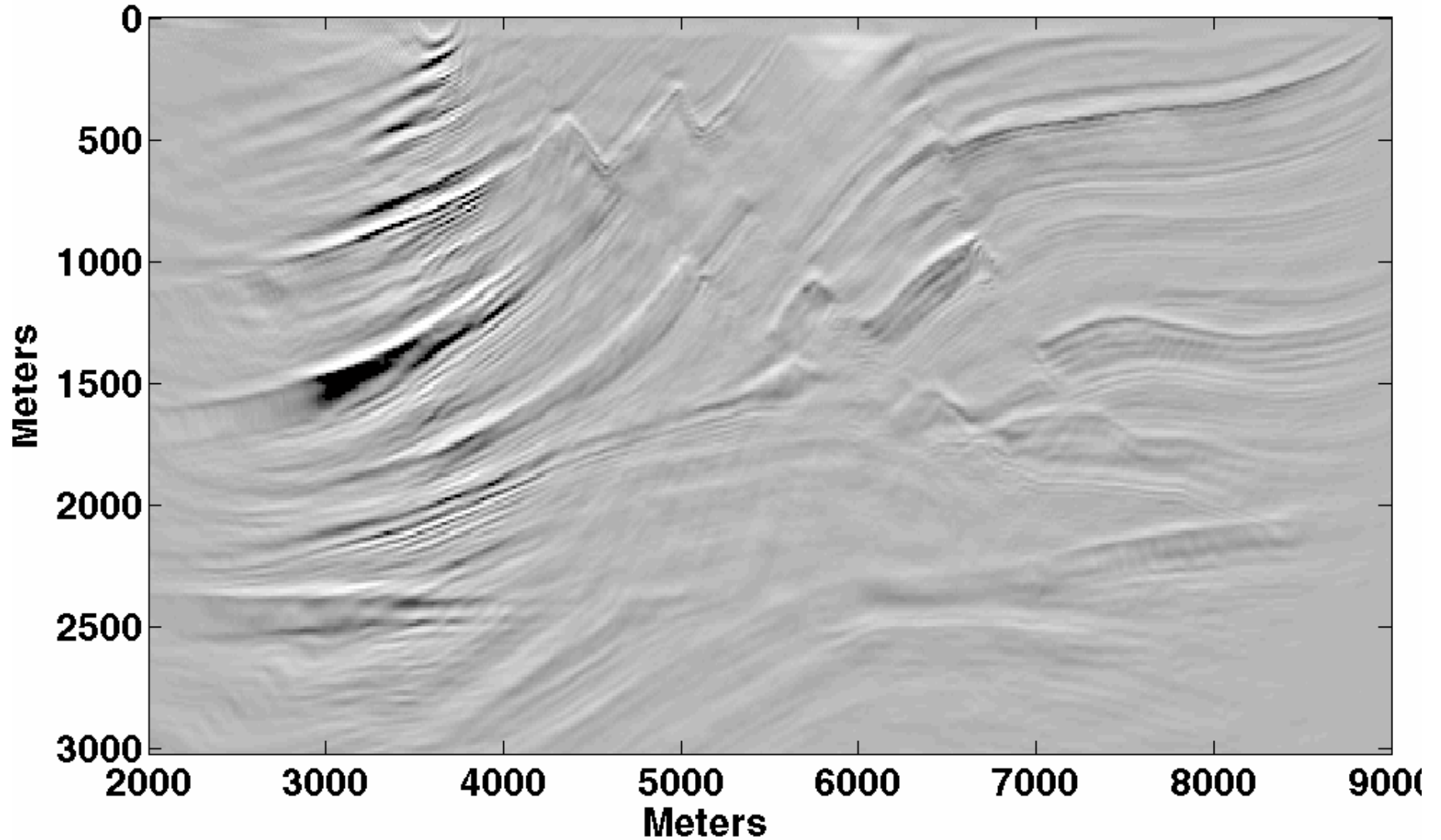
FOCI Pre-Stack Migration

Shot 30



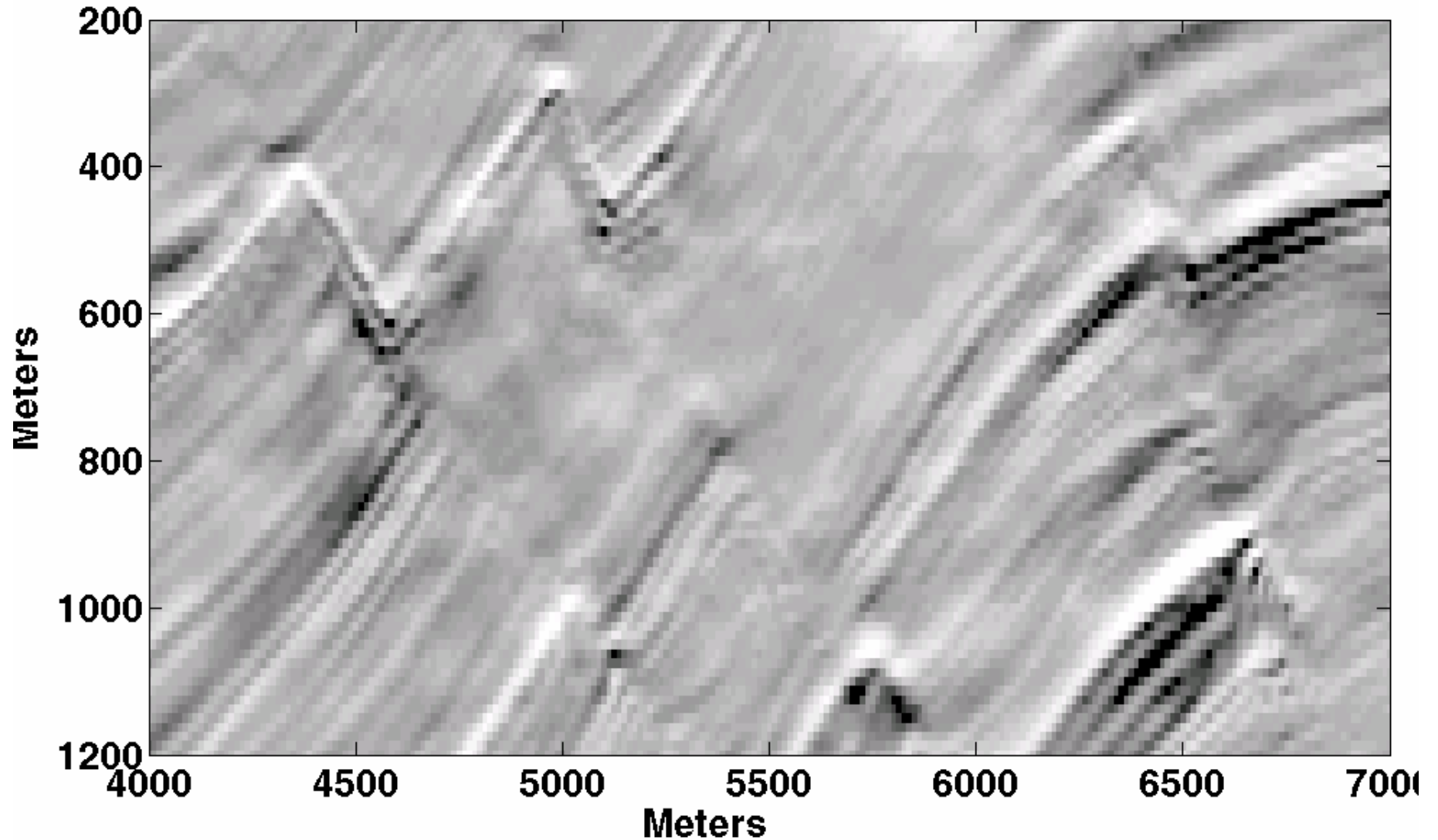
FOCI Pre-Stack Migration

Stack +50*Shot 30

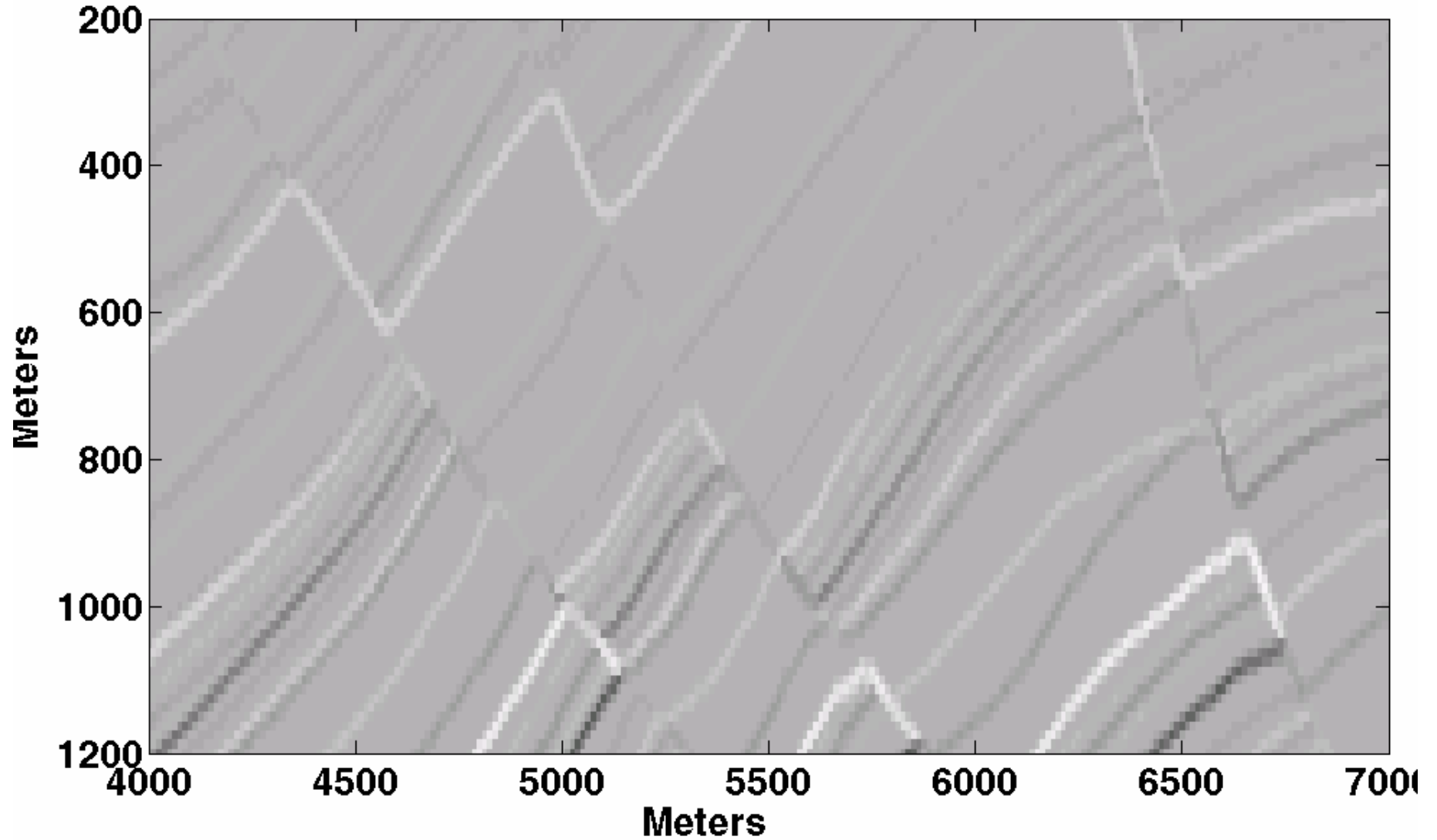


Detail of Pre-Stack Migration

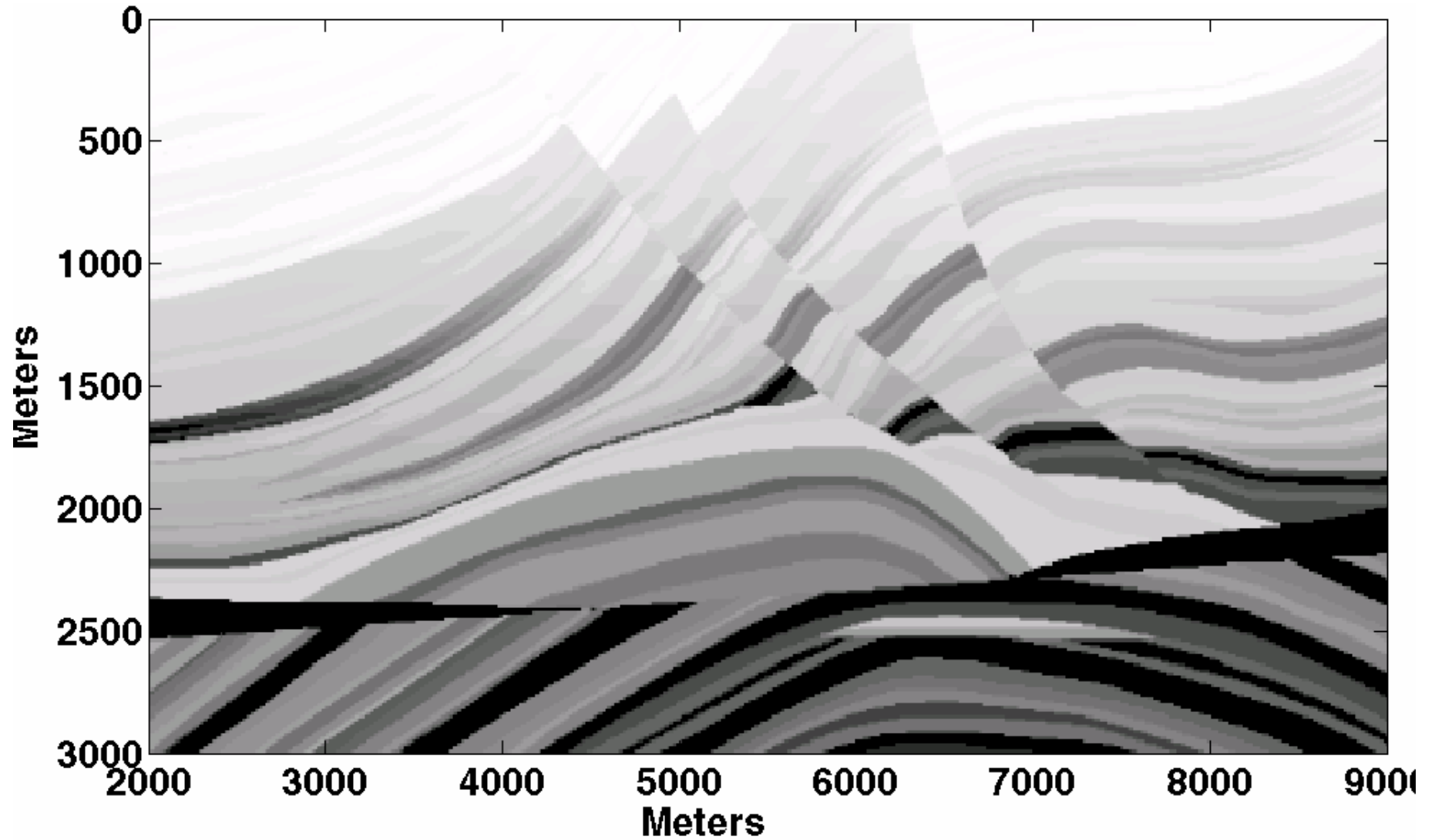
Deconvolution imaging condition



Marmousi Reflectivity Detail

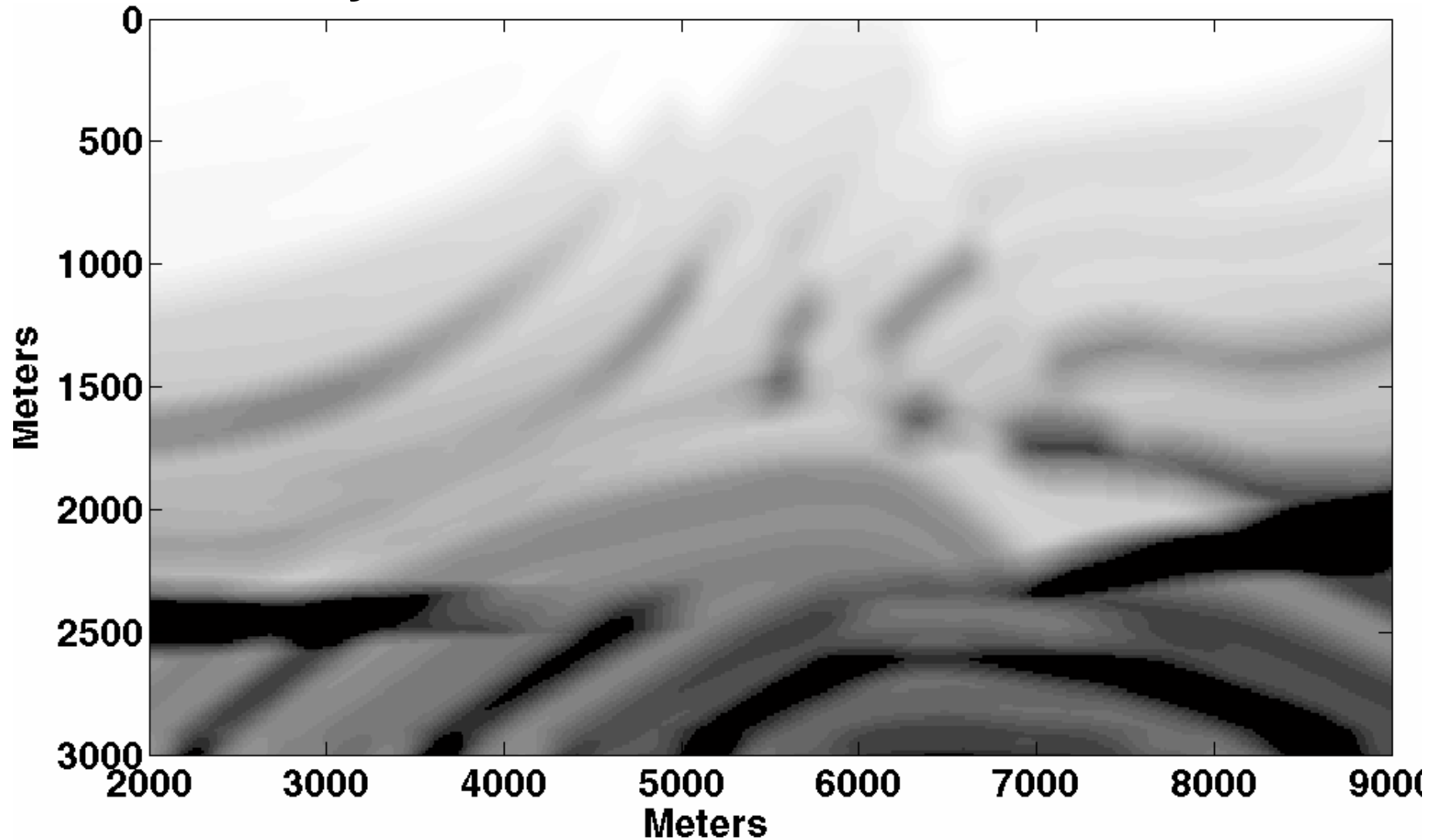


Marmousi Velocity Model



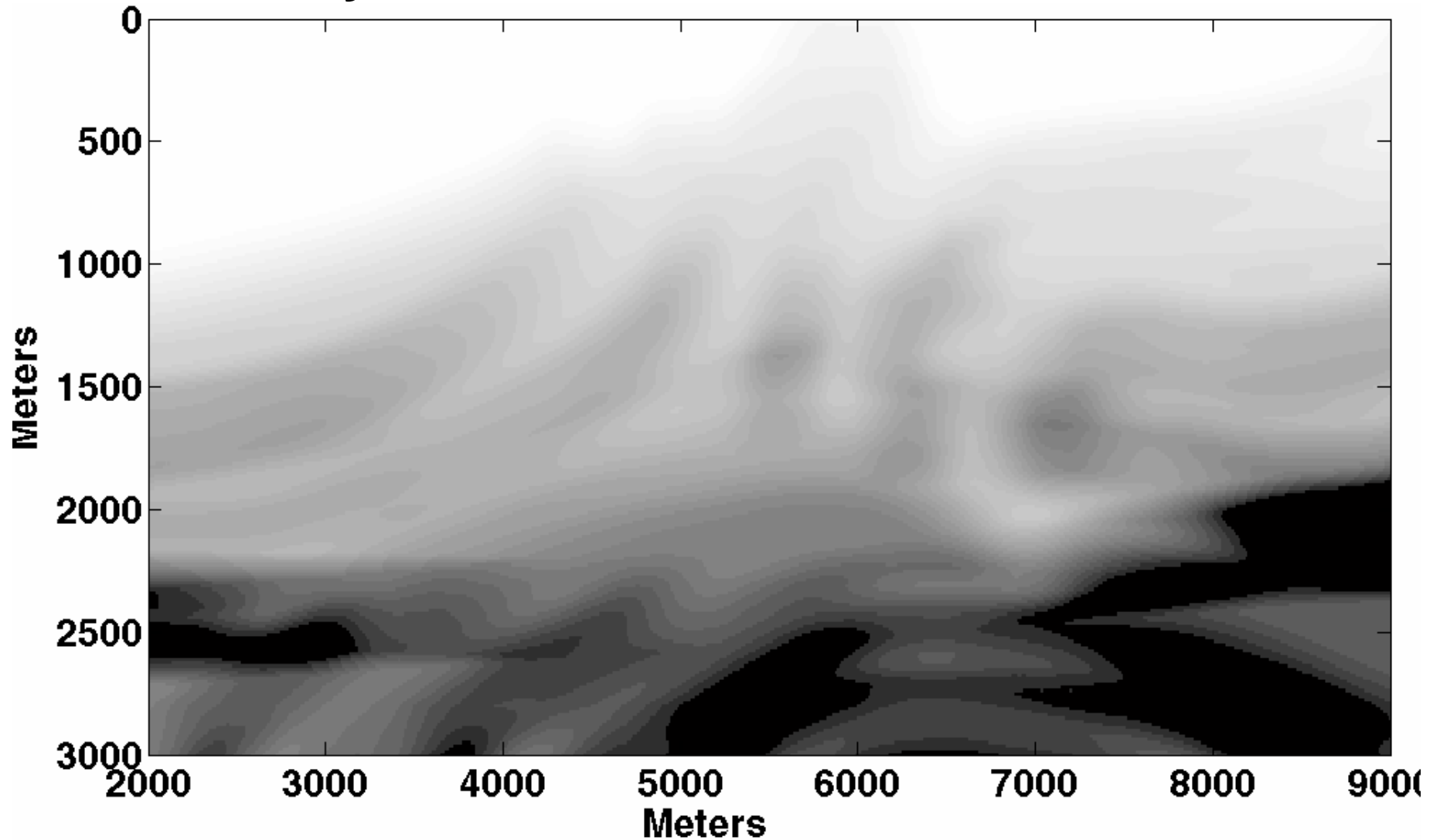
FOCI Pre-Stack Migration

Velocity model convolved with 200m smoother



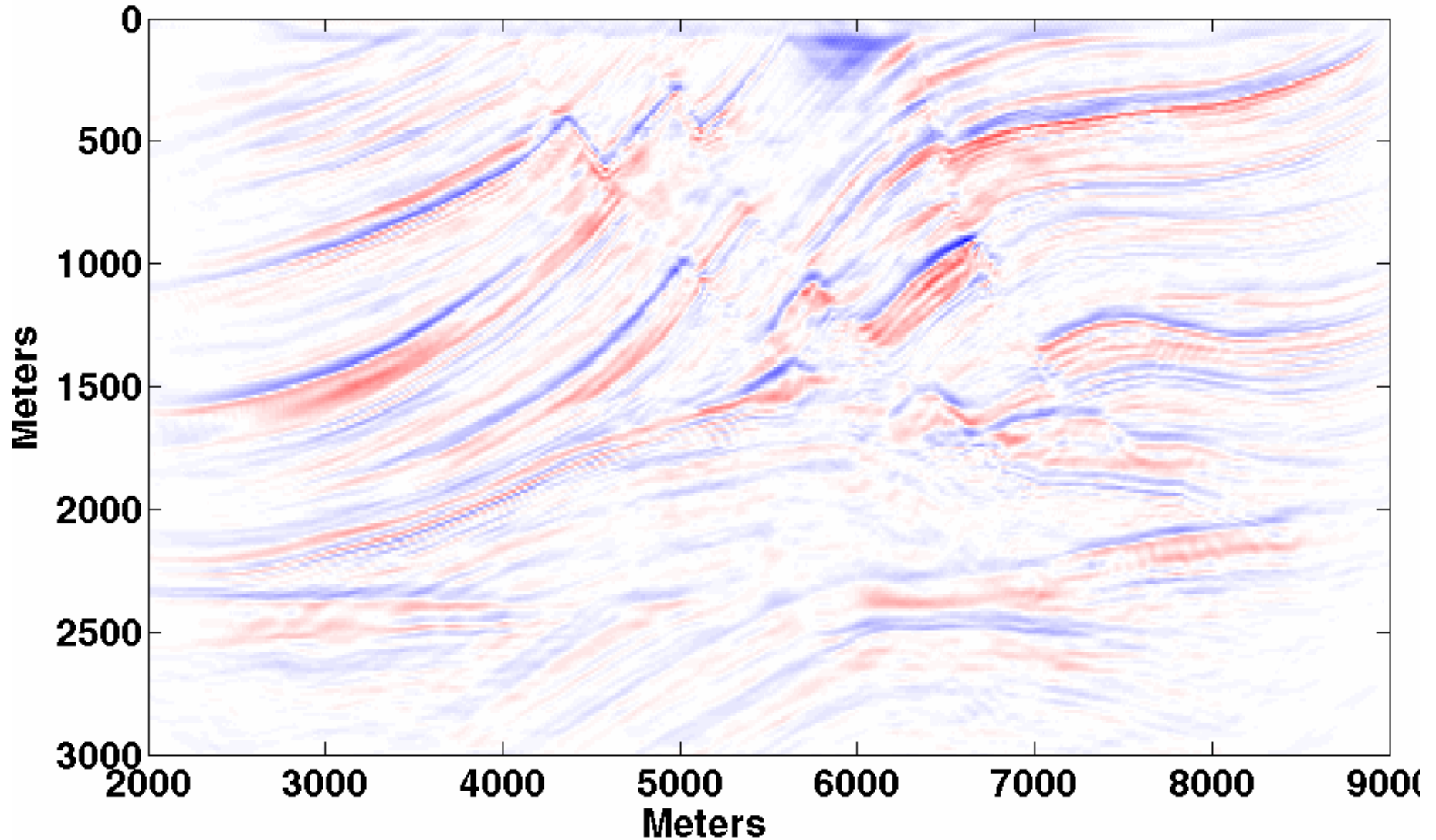
FOCI Pre-Stack Migration

Velocity model convolved with 400m smoother



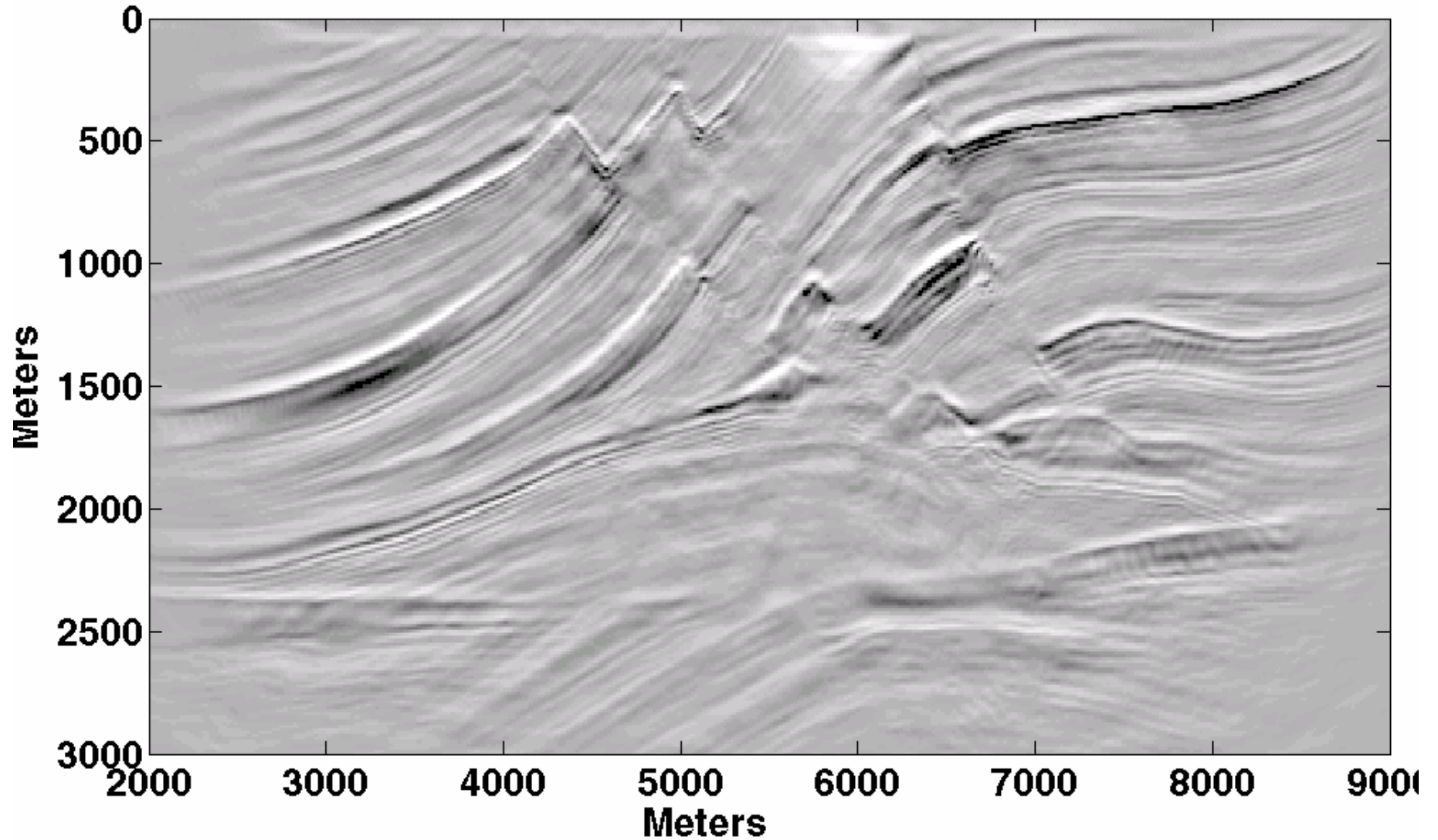
FOCI Pre-Stack Migration

Exact Velocities



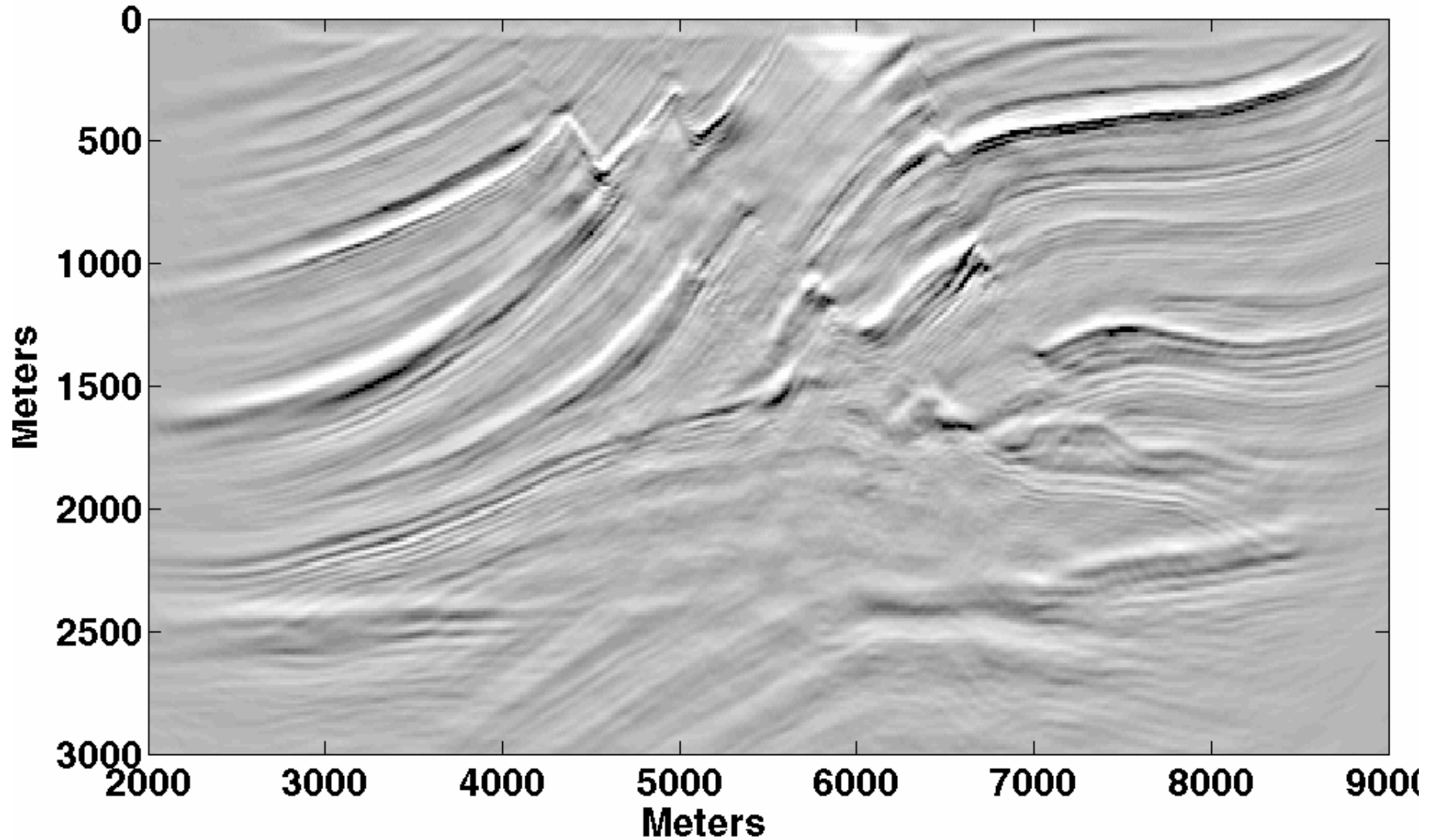
FOCI Pre-Stack Migration

Exact Velocities



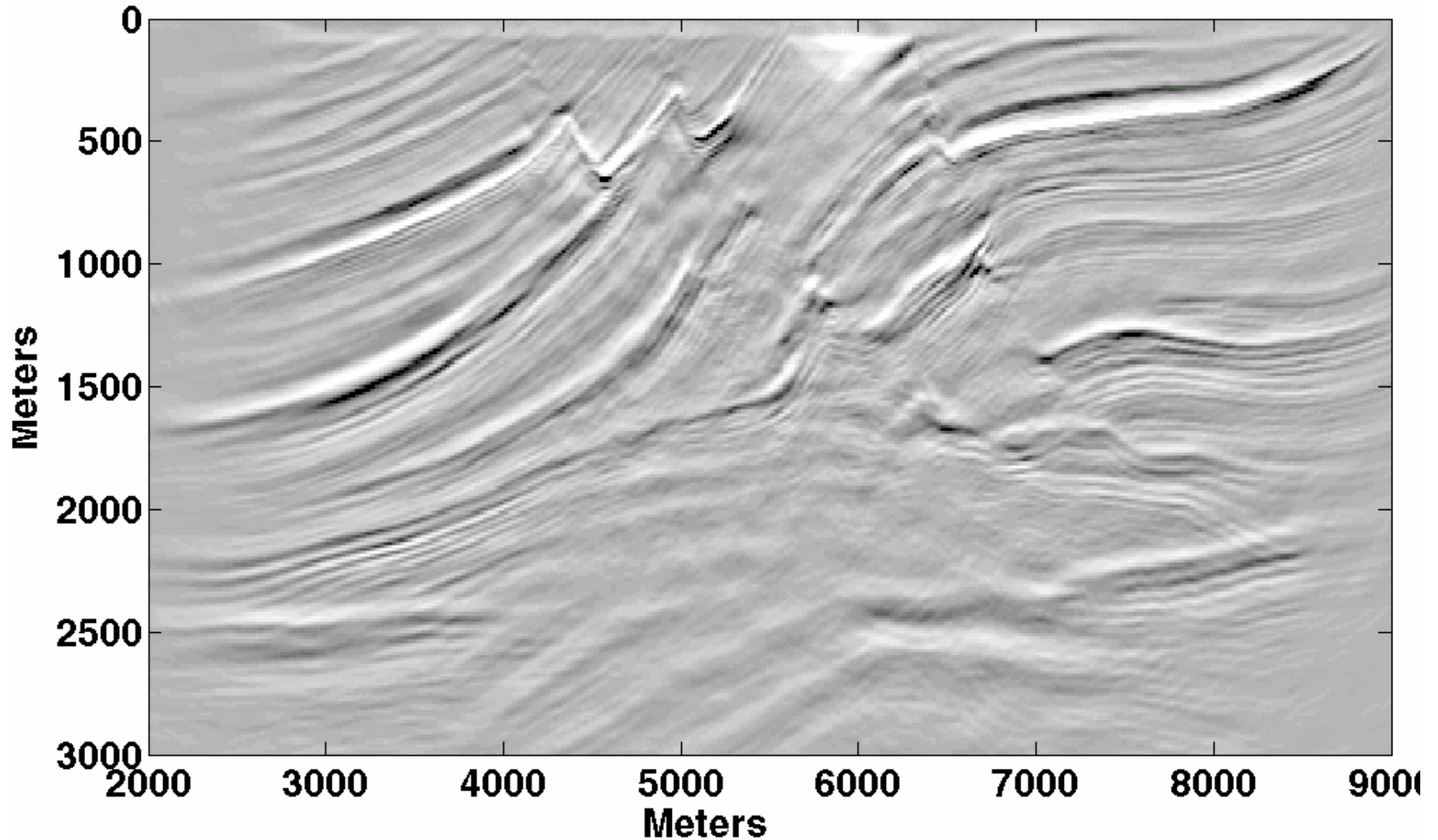
FOCI Pre-Stack Migration

Velocities smoothed over 200m



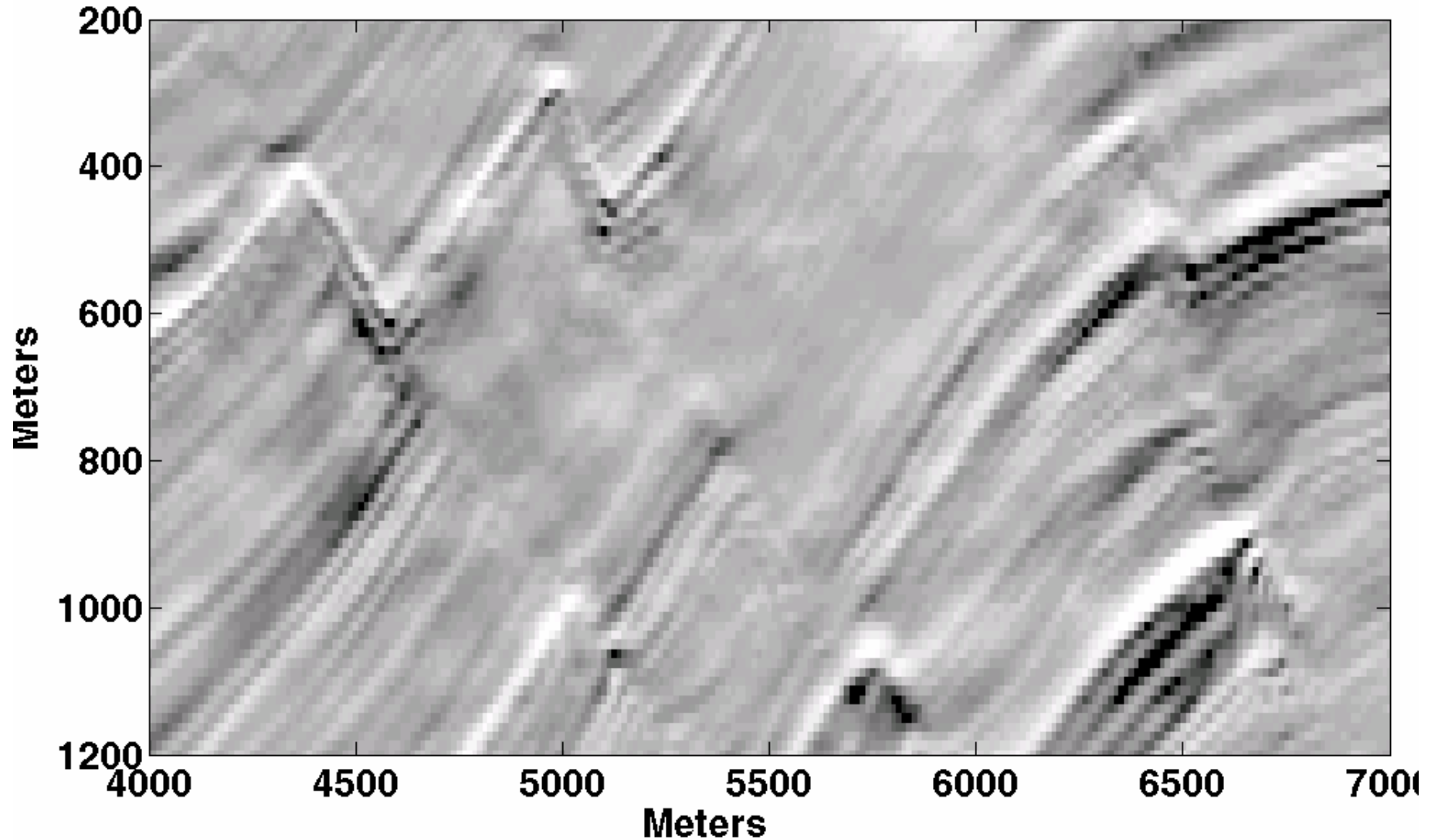
FOCI Pre-Stack Migration

Velocities smoothed over 400m



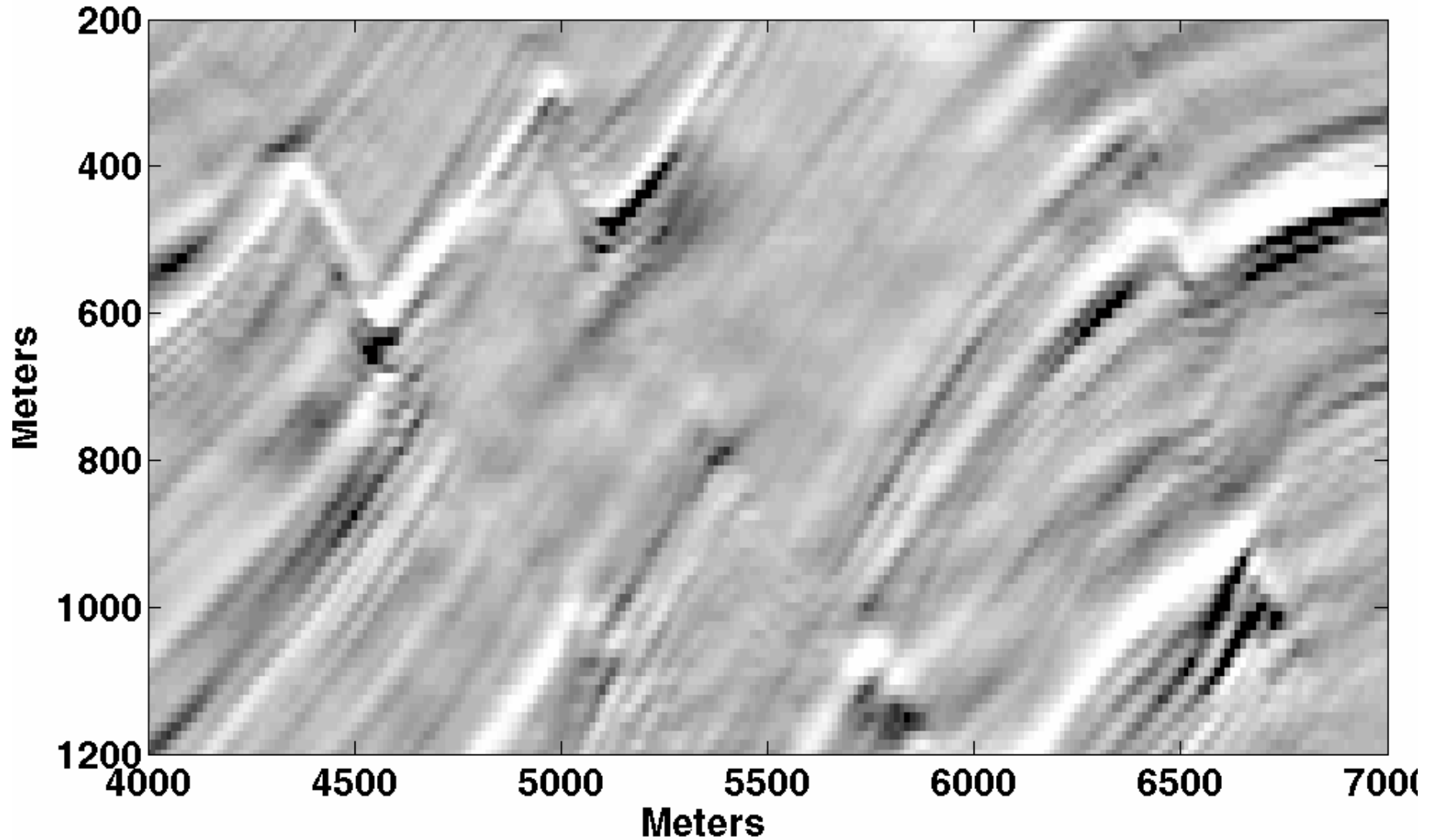
Detail of Pre-Stack Migration

Exact Velocities



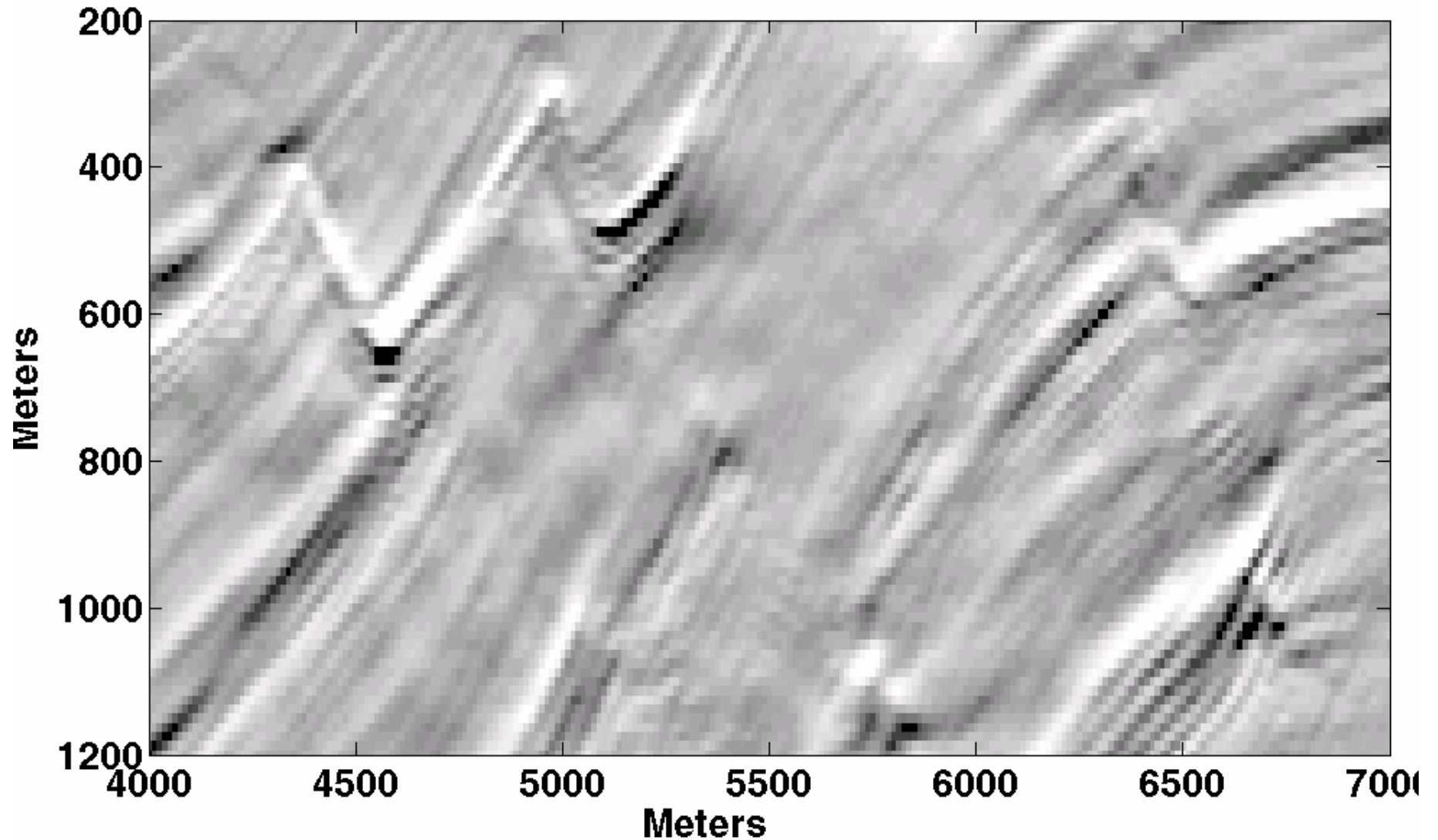
Detail of Pre-Stack Migration

Velocities smoothed over 200m



Detail of Pre-Stack Migration

Velocities smoothed over 400m



Run times

Full prestack depth migrations of Marmousi on a single
2.5GHz PC using Matlab code.

20 hours for the best result

1 hour for a usable result

Conclusions

Explicit wavefield extrapolators can be made local and stable using Wiener filter theory.

The FOCI method designs an unstable forward operator that captures the phase accuracy and stabilizes this with a band-limited inverse operator.

Reducing evanescent filtering increases stability.

Spatial resampling increases stability, improves operator accuracy, and reduces runtime.

The final method appears to be $\sim O(N \log N)$.

Very good images of Marmousi have been obtained.

Research Directions

Better phase accuracy.

Extension to 3D.

Extension to more accurate wavefield extrapolation schemes.

Migration velocity analysis.

Development of C/Fortran code on imaging engine.

Acknowledgements

We thank:

Sponsors of CREWES

Sponsors of POTSI

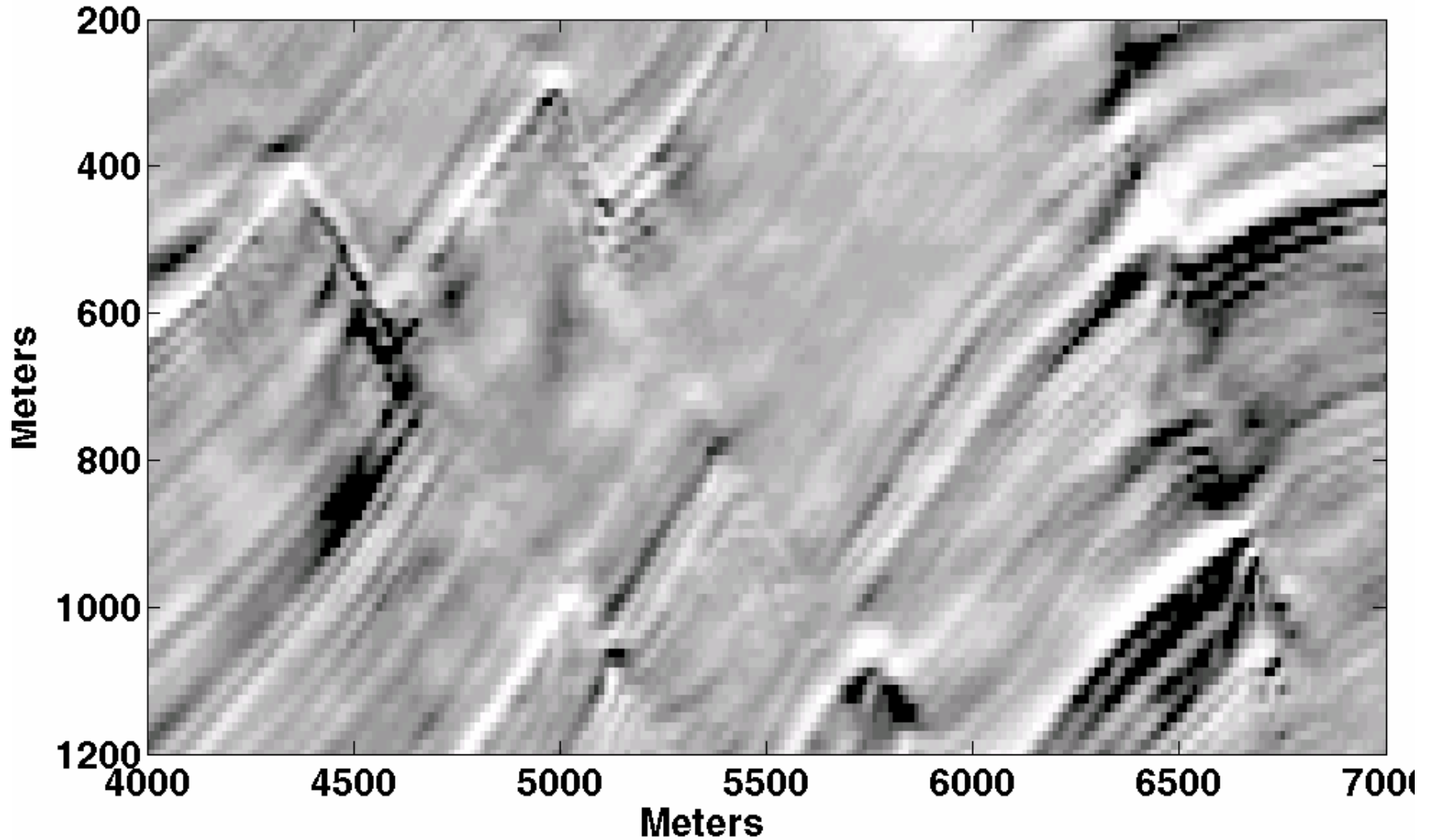
NSERC

MITACS

PIMS

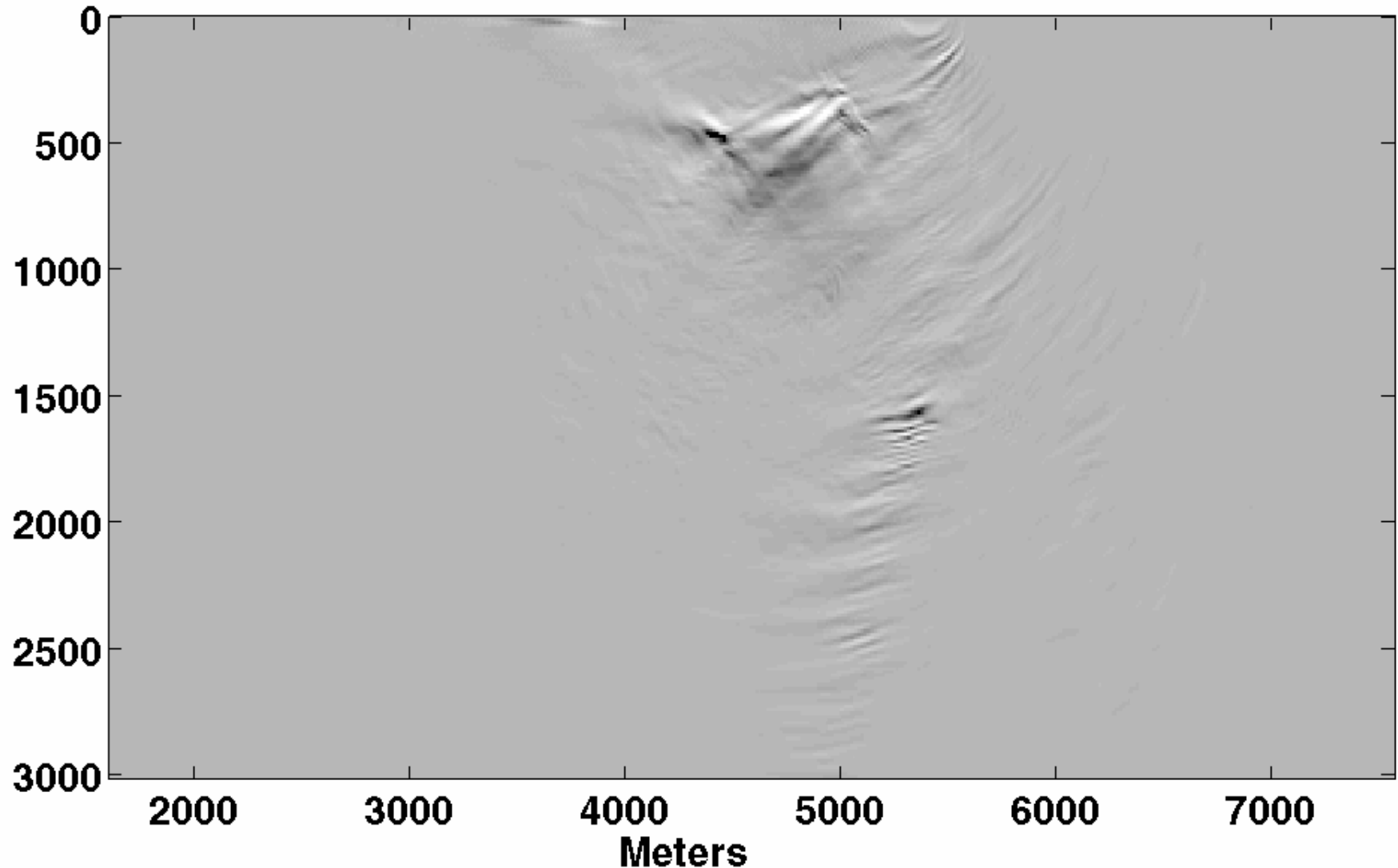
A US patent application has been made for the FOCl process.

Detail of Pre-Stack Migration



FOCI Pre-Stack Migration

nfor=21, ninv=31, nwin=0, deconvolution imaging condition
With enhanced evanescent filtering



FOCI Pre-Stack Migration

nfor=21, ninv=31, nwin=0, deconvolution imaging condition
Previous evanescent filtering

